Waste Management

Petrography of Construction and Demolition Waste (CDW) from Abruzzo Region (Central Italy)

--Manuscript Draft--

Manuscript Number:	WM-21-51
Article Type:	Full Length Article
Section/Category:	Waste Generation and Characterization
Keywords:	CDW (construction and demolition waste); Abruzzo region (Italy); XRPD; XRF; Recycling
Corresponding Author:	Antonio Galderisi ITALY
First Author:	Antonio Galderisi
Order of Authors:	Antonio Galderisi
	A. Galderisi
	G. Iezzi
	G. Bianchini
	Eleonora Paris
	Jorge de Brito
Abstract:	The density, colour and texture, plus mineral and chemical features of 18 ceramic-like CDW samples from the Abruzzo region (Central Italy) were characterised. The concretes, natural stones, tiles, roof-tiles, bricks and perforated bricks are either aphanitic to porphyric. Concretes and natural stones are grey to white and tend to be > 2.0 g/cm ^{3}; the masonries are brown to reddish and close to < 2.0 g/cm ^{3}. Concrete and natural stone are rich to exclusively made up of calcite, with high amounts of CaO (> 40 wt.%) and LOI (volatiles, CO_2 + H_2O). The masonries are instead calcite-, CaO- (< 25 wt.%) and LOI-poor (< 8 wt.%) but enriched in SiO_2 (45 to 70 wt.%), quartz and/or cristobalite, with significant amount of Al_2O_3 (12 to 20 wt%). S and Cl contents are similar among concrete, bricks and perforated bricks. Some CDW sample is susceptible to release relative high Cr content. The petrography of these CDW concretes are similar among geographical areas with abundance of limestones used like aggregates. In limestone-poor areas CDW are SiO_2 - and Al_2O_3 -rich, reflecting the prevalence using of masonry and/or silicate-rich construction materials. Therefore, each geographical area results in a peculiar petrography of CDW; it must be known for appropriate treatment and sorting methods, and especially for reusing applications. Indeed, in-depth knowledge of mesoscopic, physical and petrographic features is the basis for improving the CDW upcycling reuse.
Suggested Reviewers:	Giuseppe Bonifazi giuseppe.bonifazi@uniroma1.it For many years, his research team has been working in the field of characterization of Construction and Demolition Wastes through the use of HyperSpectral Imaging analysis methodologies.
	Petros Koutsovitis pkoutsovitis@upatras.gr Currently, he carries out research on Construction and Demolition Wastes with an approach similar to that used in the proposed manuscript, in particular for the analysis methodologies used.
	Valeria Corinaldesi v.corinaldesi@univpm.it Expert in building materials, in the reuse of Construction and Demolition Wastes for new materials, interaction of construction waste with the environment.

From the corresponding author Dr. Antonio Galderisi

To the Editor(s) of Waste Management

Dear Editor(s),

here enclosed please find the manuscript entitled "**Petrography of Construction and Demolition Waste (CDW) from Abruzzo Region (Central Italy)**" by Galderisi, Iezzi, Bianchini, Paris and de Brito.

According to the topic of our investigation, we would like to submit this contribution to your first-rank international journal. This study focuses on the physical (density and colour) and petrography of the Construction and Demolition Waste (CDW), the most abundant end of life materials worldwide (30-35% by weight of all waste). The studied CDW were sampled in the Abruzzo region (Central Italy); this region is representative of many geographical and geological areas of the Mediterranean and of their construction materials. In parallel, this region suffered several destructive earthquakes in the last years, producing significant deaths and rubbles.

An important but still poor investigated and known aspect for the effective recycle of CDW is their chemical and mineralogical attributes. To fill this gap of knowledge the most representative CDW samples from Abruzzo were investigated *via* X-Ray Powder Diffraction (XRPD) and X-Ray Fluorescence (XRF) to derive their chemical and mineralogical compositions. In addition, the potential release of toxic elements from them were also investigated. The attained outcomes were then compared with the few data available in the international literature, to show similarities and differences with those sampled in Abruzzo.

This study shows a general protocol to analyse the petrography of CDW worldwide, as well as possible methods to sort them in homogeneous sub-groups starting from an heterogeneous one. This study could encourage the reuse of these materials in a circular economic perspective.

We would like to suggest some possible reviewers, with a high and recognised scientific profile in the fields of materials characterisation and/or CDW:

1) Giuseppe Bonifazi (University of Roma, Italy): giuseppe.bonifazi@uniroma1.it
2) Valeria Corinaldesi (University of Marche, Italy): v.corinaldesi@univpm.it
3) Petros Koutsovitis (University of Patras): pkoutsovitis@upatras.gr
4) Weslei Monteiro Ambrós (Universidade Federal do Rio Grande do Sul, Brazil): weslei.ambros@ufrgs.br
5) Rosario García-Giménez (Universidad Autónoma de Madrid, Spain): rosario.garcia@uam.es
6) Guido Ventura, (INGV-Roma, Italy): guido.ventura@unich.it

We hope that everything has been done according with the recommendation of the journal, and we are grateful to you in advance for the editorial handling.

Best regards, Antonio Galderisi and co-authors

Highlights

- Petrography of Construction and Demolition Wastes (CDWs)
- Analysis and characterization of CDWs through X-ray Powder Diffraction (XRPD) and X-Ray Fluorescence (XRF) analysis methodologies
- Proposal general protocol to analyse the petrography of CDW worldwide

Petrography of Construction and Demolition Waste (CDW) from Abruzzo Region (Central Italy)

Galderisi A. *[1,2], Iezzi G. [1,3], Bianchini G. [4], Paris E. [5] and de Brito J. [6]

[1] Dipartimento INGEO (Ingegneria & Geologia), Università di Chieti-Pescara 'G. d'Annunzio', Chieti, Italy

[2] Istituto di Geologia Ambientale e Geoingegneria IGAG - Centro Nazionale delle Ricerche CNR Rome, Italy

[3] Istituto Nazionale di Geofisica e Vulcanologia INGV, Rome, Italy

[4] Dipartimento di Fisica e Scienze della Terra, Università di Ferrara, Ferrara, Italy

[5] Scuola di Scienze e Tecnologie, sez. Geologia, Università di Camerino, Camerino, Italy

[6] CERIS, Instituto Superior Técnico, Universidade de Lisboa, Lisboa, Portugal.

*corresponding author: antonio.galderisi@unich.it, g.iezzi@unich.it

Abstract

The density, colour and texture, plus mineral and chemical features of 18 ceramic-like CDW samples from the Abruzzo region (Central Italy) were characterised. The concretes, natural stones, tiles, roof-tiles, bricks and perforated bricks are either aphanitic to porphyric. Concretes and natural stones are grey to white and tend to be > 2.0 g/cm^3; the masonries are brown to reddish and close to < 2.0 g/cm^3. Concrete and natural stone are rich to exclusively made up of calcite, with high amounts of CaO (> 40 wt.%) and LOI (volatiles, CO_2 + H_2O). The masonries are instead calcite-, CaO- (< 25 wt.%) and LOI-poor (< 8 wt.%) but enriched in SiO_2 (45 to 70 wt.%), quartz and/or cristobalite, with significant amount of Al_2O_3 (12 to 20 wt%). S and Cl contents are similar among concrete, bricks and perforated bricks. Some CDW sample is susceptible to release relative high Cr content.

The petrography of these CDW concretes are similar among geographical areas with abundance of limestones used like aggregates. In limestone-poor areas CDW are SiO_2- and Al_2O_3-rich, reflecting the prevalence using of masonry and/or silicate-rich construction materials. Therefore, each geographical area results in a peculiar petrography of CDW; it must be known for appropriate treatment and sorting methods, and especially for reusing applications. Indeed, in-depth knowledge of mesoscopic, physical and petrographic features is the basis for improving the CDW upcycling reuse.

Keywords: CDW (construction and demolition waste), Abruzzo region (Italy), XRPD, XRF, recycling.

Introduction.

Construction and demolition waste (CDW) are all solid materials deriving from civil engineering works (buildings, roads, bridges, etc.), as well as from their demolition, restoration and/or collapse due to natural or man-induced causes (e.g. earthquakes, landslides). CDW are extremely abundant in both the EU and Italy, as summarised in Figs. S1a, b. They are mainly composed of inert materials, i.e. "ceramic-like" solids (concrete, mortars, cement, tiles, roof-tiles, bricks, natural stone, etc.), plus asphalt, metals, plastics, textiles, wood, glass, RAEE (waste of electric and electronic equipment), soils and/or dredging materials (Figs. S1c, d) (e.g. Blengini & Garbarino, 2010; Vitale et al., 2017). Commonly, inert ceramic-like CDW (hereafter only CDW) are collected separately from asphalt, wood, plastics, metals, and textiles waste, and/or routinely separated from them (Martín-Morales et al., 2011; Di Maria et al., 2013; Ulsen et al., 2013; Bonifazi et al., 2017a; Neto et al., 2017; Ambros et al., 2019) (Fig. S1d).

By contrast, the separation of heterogeneous CDW in relative homogeneous sub-populations is complex and expensive. In turn, their physico-mechanical and petrographic (meaning as chemical, mineralogical and textural attributes) features are frequently variable in time and space determining poorly measurable and predictable behaviours (de Brito et al., 2005; Gonçalves & de Brito, 2010; Coelho & de Brito, 2013). This heterogeneity strongly limits their reusing; frequently, new construction materials prepared with them may be characterized by low quality mechanical properties (Coelho & de Brito, 2013). As a result, most CDW are low price materials, downcycling reused mainly for road foundations, foundation slab, and cavity fillings (Coelho & de Brito, 2013; Di Maria et al., 2013 and 2016; Gálvez-Martos et al., 2018).

From a petrographic and materials science perspective, CDW are multi-phases solids made up of silicate and/or carbonate minerals and glasses. The petrography of construction materials is still poorly investigated and known: specifically, only a limited number of studies worldwide investigated their mineralogical and/or chemical (i.e. petrographic) features (Bianchini et al., 2005 and 2020; Limbachiya et al., 2007; Rodrigues et al., 2013; Alexandridou et al., 2014; Komnitsas et al., 2015; Moreno-Perez et al., 2018; Panizza et al., 2018; Frias et al., 2020). This is a significant limitation for recycling since the petrography of CDW inevitably reflects available lithotypes (rocks), architectural and historical styles, as well as national regulations of a geographical area. Therefore, the petrographic attributes of CDW of each region have to be known to plan their possible reuse.

In this paper, the most abundant and frequent ceramic-like CDW randomly sampled in the Abruzzo region, Central Italy, were investigated. To the best of the authors' knowledge, they were never investigated, although this region can be representative of several Italian (Apennines, Dolomites) and Mediterranean (Greece, southern France, Albania) geographical and geological areas, mainly characterised by limestone, sandstone and claystone lithotypes, including their incoherent to poorly lithified dismantled and re-sedimented deposits (Geological Map at 1:500 000 scale; Vola et al., 2011). Moreover, the Abruzzo region and its surroundings areas were repeatedly hit by earthquakes in the last decades, causing the loss of many human lives and accumulation of huge amounts of CDW rubbles in the most damaged cities (Galli et al., 2017).

The aim of this study is to characterise common and representative single CDW samples from the Abruzzo region via their mesoscopic, physical features and mineralogy (crystalline and non-crystalline attributes) by X-Ray Powder Diffraction (hereafter XRPD) analysis. Then, a sub-set of them was also characterised with X-Ray Fluorescence Wavelength Dispersive Spectroscopy (hereafter XRF-WDS) to quantify the chemical features. In addition, the potential release of chemical species from this CDW was also assessed. Finally, the petrographic features of the CDW from Abruzzo have been compared with those from other geographical and geological regions.

Materials and methods

Mesoscopic and physical features. The 18 single CDW samples considered here were collected in various cities and towns of the Abruzzo region; they are the most representative, frequent and common construction waste materials. The CDW samples were classified in several groups according to their mesoscopic appearance and commercial using: concrete (4), natural stone (Apennines carbonate) (2), bricks (3), tiles (3), roof tiles (3) and perforated bricks (3) (Table S1 and Fig. S2). In Fig. S2, the diameter of the mortar is about 5 cm.

The mesoscopic colour of the samples refers to bulk and as-received appearance, while the powder colour is that obtained after grinding a portion of it for further analyses (see below). The texture refers to the classical petrographic observations and discrimination of grains in rocks used in Earth Sciences (Merico et al., 2020; Giuliani et al., 2020), such as: i) aphanitic and phaneritic for grains invisible (< some tens of µm) and visible (> some tens of µm) by the naked-eye or an optical lens (10 X), respectively. The porphyric texture refers to phaneritic grains immersed in an aphanitic matrix. The density was measured by weighing a relatively large piece (some cm^3) of each sample and measuring the volume with a water bath (graduated Becker).

XRPD (X-ray powder diffraction). The crystalline and non-crystalline phases were analysed *via* XRPD. For each bulk sample, about 10/20 g were grinded under alcohol using an electrical grinder: the produced powders had crystallite sizes of few hundreds of μm. About 2/3 g of each of these powders were dried and further grinded for 10 minutes again under alcohol, using an agate pestle and mortar. The final powdered samples were homogeneous and with crystallites sizes below 10 μm. Each fine powder was mounted into a cylindrical nominally zero-background Si sample holder, with a random distribution of crystallites. Using a zero-background Si sample holder allows qualitatively detecting the presence of non-crystalline phases.

Each powdered sample was analysed with a SIEMENS D-5000, with a Bragg-Brentano θ-2θ configuration, equipped with CuKα radiation and a Ni filter. Each XRPD pattern was collected from 4 to 80° of 2θ, with a step scan of 0.02° and counting time of 4 s per step. Each XRPD pattern was thus recorded in approximately 8 hours. The obtained XRPD patterns were first checked for the presence of non-crystalline content by observing some background shoulder (Walter et al., 2013; Boncio et al., 2020). Then, the Bragg reflections were assigned by search-match comparisons to crystalline standards contained in the inorganic crystal structure database (ICSD) (Boncio et al., 2020). The search-match identification of measured Bragg reflections started from the most intense peaks; the XRPD standards that better reproduce either the 2θ positions or the relative intensities of measured Bragg reflections were used to identify the minerals in each sample (Fig. 1).

The abundance of crystalline phases (wt%), was semi-quantitatively evaluated using the RIR (reference intensity ratio) method (Hubbard and Snyder, 1998; Johnson and Zhou, 2000; Chipera and Bish, 2013; Boncio et al., 2020). The RIR method used here is implemented in the software package “Match! version 3.9.0” (Crystal Impact, 2019). The RIR compares the intensity scaling factor of each mineralogical phase (I) with a “virtual” corundum crystalline phase (Icor.), which is not necessarily present in the XRPD patterns. The ratio “I/Icor.” is then used for assessing semi-quantitatively the content (wt%) of each crystalline phase (Table S2).

XRF-WDS. Based on the XRPD outcomes, the chemical compositions of 11 samples (MPA-10, MPA-18, MPA-04, MPA-14, MPA-07, MPA-11, MPA-09, MPA-16, MPA-01, MPA-05 and MPA-15) were obtained using a XRF-WDS analysis (Table S3 and S4). The major, minor and trace elemental features were obtained both using a Philips PW 1480 spectrometer, calibrated using external standards by Chunshu et al. (1996) following the procedure defined by Gazzulla Barreda et al. (2016), and an ARL Advant-XP spectrometer, following the full matrix correction method proposed by Lachance and Traill (1966). The accuracy is < 5% for major oxides, and < 10% for trace element. Volatiles were determined by loss on ignition (LOI) at 1000 °C.

Leaching test. Leaching tests were also performed (Table S5). The adopted leaching protocol was modified from the UNI EN 12457-Part 2 (2004) and also reported in Bianchini et al. 2020. Briefly, 1 g of CDW powder was soaked with 10 ml of deionised water for 24 h and the obtained solution was centrifuged at 3000 rpm for 10 min and filtered at 45 µm (Minisart®NML syringe cellulose acetate filters). The composition of leachates (expressed in mg/l) was obtained by inductively coupled plasma mass spectrometry (ICP-MS) using a Thermo X-series spectrometer instrument on samples previously diluted 1:5 by deionised Milli-Q water (resistivity of ca. 18.2 MΩ x cm). Instrumental calibration was carried out using certified solutions and a known amount of Re and Rh was also introduced in each sample as an internal standard. Accuracy and precision were determined using several international reference standards, being lower than 10% of the measured value, with detection limits in the order of 0.001 mg/l.

Results

Mesoscopic texture. The mesoscopic appearance and texture, as well as density of the four concrete, two natural stone, three brick, three tile, three roof tile and three perforated brick CDW samples are reported in Table S1 and displayed in Fig. S2. The colour of bulk as-received concrete is invariably pale grey and that of natural stone is either grey or white. All the other materials, i.e. tiles, roof tiles, bricks and perforated-bricks, except the sample MPA-07, are coloured (Table S1 and Fig. S2).

The MPA-03, MPA-10, MPA-13 and MPA-18 concrete samples are all characterized by a porphyric texture, with large and visible clasts (aggregate) immersed in an aphanitic matrix made of cementitious binders. The natural stones are either aphanitic (MPA-08) or porphyric (MPA-19) (Table 2). The bricks MPA-02 and MPA-04 are porphyric and the MPA-14 aphanitic, the MPA-07, MPA-11 and MPA-17 tiles are invariably aphanitic, while the roof tiles MPA-09 and MPA-12 are aphanitic and only the MPA-16 is porphyric (Table S1). Finally, the two perforated bricks MPA-01 and MPA-05 are aphanitic and the MPA-14 is instead porphyric.

Density. The density of concrete varies between 2.02 and 2.49 g/cm^3, and that of natural stone between 2.1 and 2.74 g/cm^3. The density of the four bricks ranges from 1.7 to 2.25 g/cm^3, that of the three tiles from 1.83 to 2.3 g/cm^3, that of roof tiles from 1.71 to 2.22 g/cm^3 and that of the three perforated bricks is invariably < 2 g/cm^3, i.e. between 1.73 and 1.94 g/cm^3 (Table S1).

Crystalline (and non-crystalline) phases. The XRPD spectra are stacked in Fig. 1, as a function of groups (Table S2). A more detailed visualization of them per group is reported in Figs. S3a, b, c, d, e, f, while a comparison of the crystalline phases' content is provided in Fig. 2. All concrete samples show significant amounts of calcite and quartz and the MPA-13 and MPA-18 spectra also display illite and plagioclase. Overall, the mineralogical composition of these four concrete samples is similar, while the presence of non-crystalline phase is undetected or barely appreciable (Figs. 1 and S3a). The four concrete samples are composed of calcite with a range comprised between 56 and 88 wt.%, plus a moderate to significant amount of quartz ranging from 8 to 27 wt.%; plagioclase feldspars and illite sheet-silicates are absent or with moderate to minor contents, i.e. up to 19 and 5 wt.%, respectively (Table S2 and Fig. 2). The two stone samples are made up exclusively of calcite and free of non-crystalline materials (Figs. 1 and S3b).

The other four groups are notably different from concrete, since they are characterised by silicate crystalline phases and free of calcite, except for the roof tiles MPA-12 and MPA-16 (Table S2 and Figs. S3a, b, c, d, e, f). Quartz and cristobalite, the two SiO_2 polymorphs of SiO_2, are the most abundant crystalline phases (Table S2 and Figs. 1, S3a, b, c, d, e, f). Indeed, the non-crystalline phases cannot be characterised by XRPD, but should be also SiO_2-rich according to the broad shoulder position, the prevalent chemical system and its determination for a sub-set of samples (see below).

The bricks contain quartz, cristobalite, clinopyroxene, alkali-feldspar, plagioclase, melilite and mullite. The MPA-04 and MPA-14 samples display a given amount of non-crystalline phases, the MPA-02 and MPA-04 samples are relative similar, whereas MPA-14 is by far the most different sample from the previous two (Table S2, Figs. 1, S3c and 2).

The three perforated bricks are composed of quartz, clinopyroxene, plagioclase, biotite and melilite, and free of calcite (Figs. 1 and S3f). Their mineralogical content is relatively similar for clinopyroxene and plagioclase, ranging respectively between 12 to 26 and 7 to 14 wt.%; melilite is instead either absent or up to 24 wt.%, while quartz changes from 45 to 75 wt.% (Table S2 and Fig. 2).

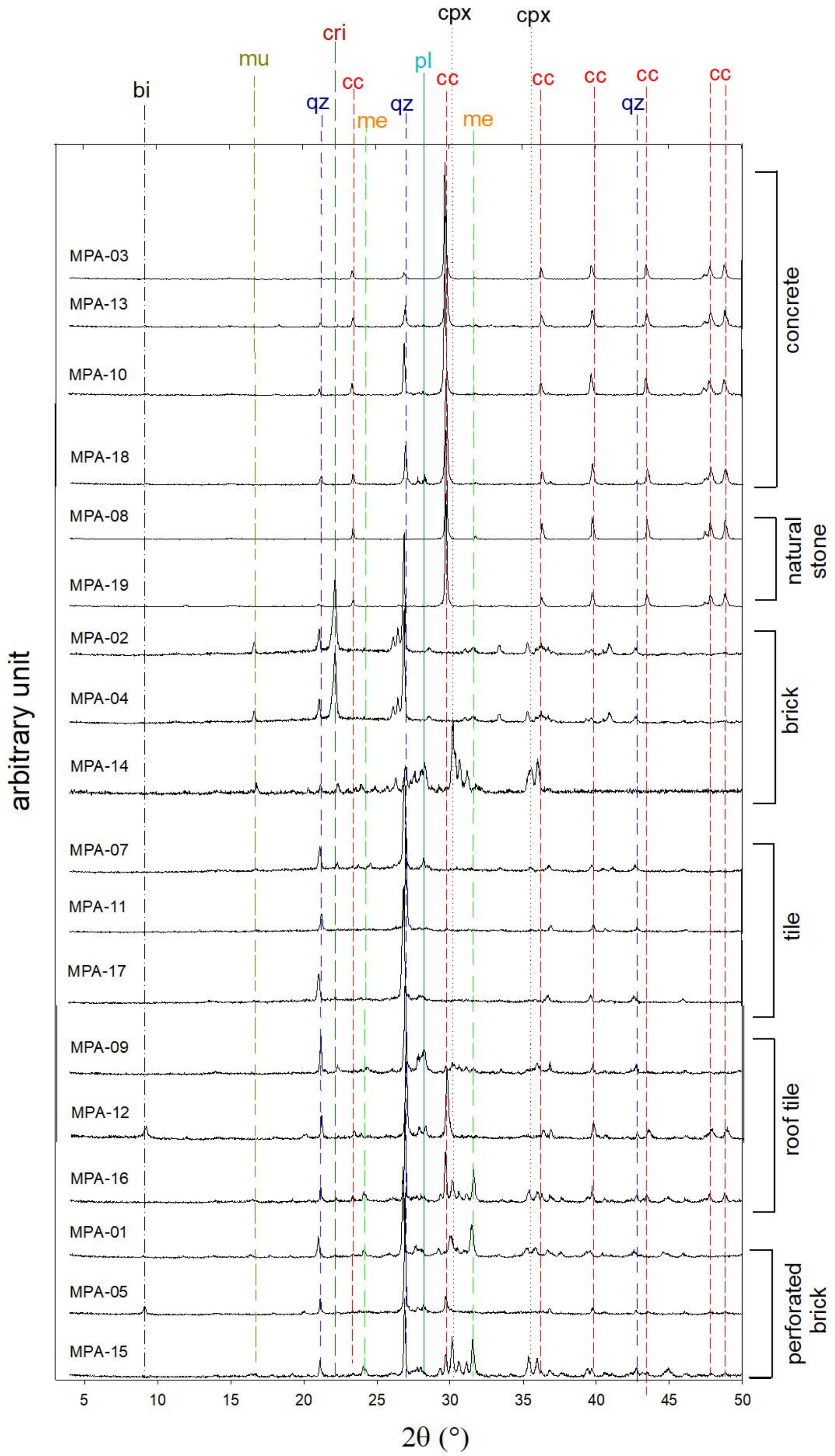

Fig. 1. Stacked XRPD patterns with indentified Bragg reflections to their corresponding crystalline standards from the ICSD database. A more detailed visualisation of these XRPD patterns is reported in Figs. S3a, b, c, d, e and f.

The three tiles are mainly composed of quartz and cristobalite, plus minor plagioclase and variable amount of non-crystalline phases, showing very similar XRPD patterns, mirroring a very close crystalline and non-crystalline content of phases (Figs. 1 and S3d). In line, they are made of 70 to 100 wt.% of quartz, an amount of cristobalite and plagioclase switching between 6 to 8 and 24 to 11wt.%, plus non crystalline phase in sample MPA-07 (Table S2 and Fig. 2).

The three roof tiles contain quartz and cristobalite, calcite, clinopyroxene, plagioclase, biotite and melilite, whilst non-crystalline phases were undetected (Figs. 1 and S3e). Overall, MPA-12 and 16 show the wt.% of very similar crystalline phases. Differently, MPA-09 has no calcite and major values of clinopyroxene and plagioclase, relative to MPA-12 and 16 (Table S2 and Fig. 2).

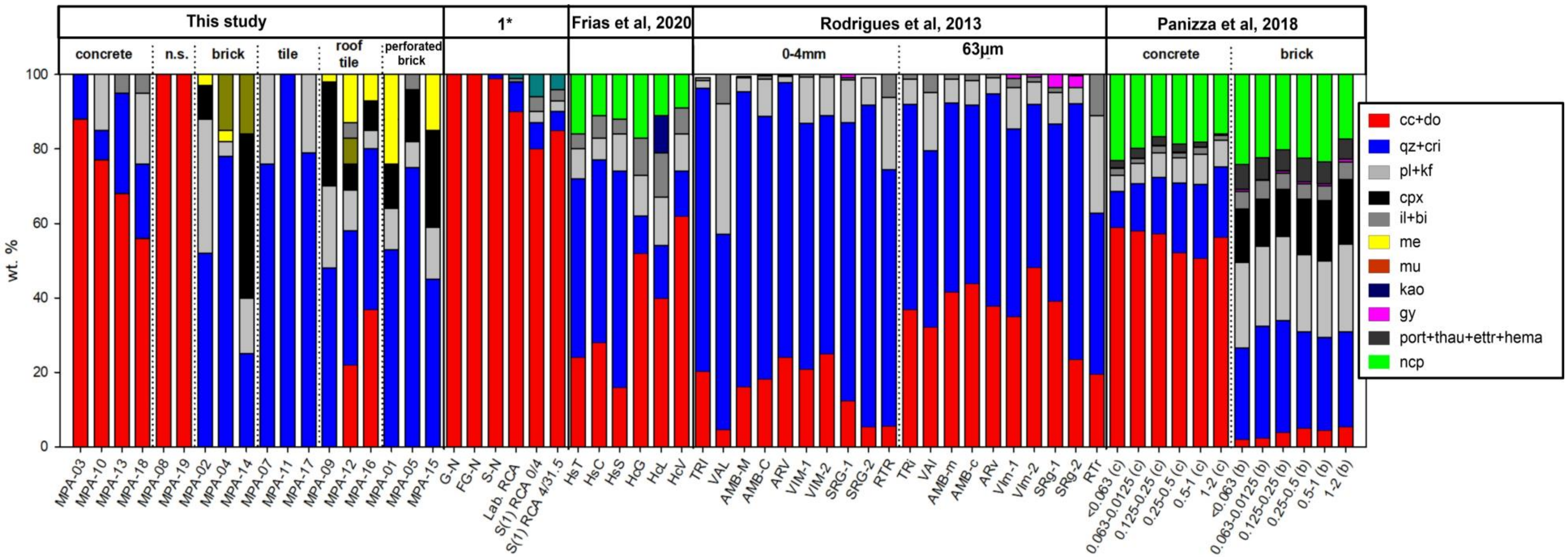

Fig. 2. Semi-quantitative content of crystalline phases (wt. %) in the Abruzzo samples (this study, Table S2).

Concrete is rich to very rich in cc, ornamental stones are made of cc only, whereas bricks, tiles, roof tiles and perforated bricks are cc-poor and -free, but rich in silicate crystalline phases. The other data from previous studies are from the following geographical regions: 1* - southern Greece (Alexandridou et al., 2014), central Spain (Frias et al., 2020), Portugal (Rodrigues et al., 2013) and Veneto region of Italy (Panizza et al., 2018). The acronyms are n.s.: natural stone, cc: calcite, do: dolomite, qz: quartz, cri: cristobalite, pl: plagioclase, kf: k-feldspar, cpx: clinopyroxene, il: illite, bi: biotite, me: melilite, mu: mullite, kao: kaolinite, gy: gypsum, port: portlandite, thau: thaumasite, ettr: ettringite, hema: hematite and ncp: non-crystalline phase

Bulk chemical composition. The major chemical species are expressed in oxide weight per cent (wt. %), while the minor and trace elemental features are reported in mg/kg (Tables S3 and S4). Since the two stone samples (Apennines limestone) are composed of calcite only (Figs. 1 and S3b), their chemical compositions are very close to $CaCO_3$ and were thus not analysed. The bulk major oxide compositions of the 11 selected samples are compared in Figs. 6 and 7.

The first important difference is the significant distinction between concrete and all the other groups. The former is very rich in CaO (> 40 wt.%) plus LOI (> 25 wt.%), with moderate amounts of SiO_2 (< 27 wt.%), poor in Al_2O_3 (< 2.5 wt.%) and with very low contents of Fe_2O_3 (< 1.5 wt.%), MgO (< 1 wt.%) and alkalis (< 0.6 wt.%) (Table S3 and Figs. 3, 4). The high content of LOI is related to the CO_2 content derived from calcite, as measured by XRPD (Table S2 and Fig. 2). Conversely, brick, tile, roof tile and perforated brick groups are invariably rich in SiO_2 (> 47 and < 71 wt.%) and Al_2O_3 (> 12 and < 20 wt.%), while relatively poor in CaO (< 24 wt. %): tiles are extremely poor in CaO (< 3 wt.%) (Table S3 and Figs. 3, 4). The other oxides are relatively abundant: notably, Fe_2O_3 is around 1.5 wt.% for tiles but approximately 5 wt.% for bricks, roof tiles and perforated bricks (Table S3 and Figs. 3, 4). A similar situation is shown by MgO and alkalis (Figs. 3, 4). The tiles are richer in Al_2O_3 and poorer in Fe_2O_3 and MgO compared to bricks, roof tiles and perforated bricks (Table S3 and Figs. 3, 4). Notably, the amounts of CaO and respective LOI of these groups show an opposite correlation, testifying that their LOI are poorly related to the content of calcite (Fig. 4).

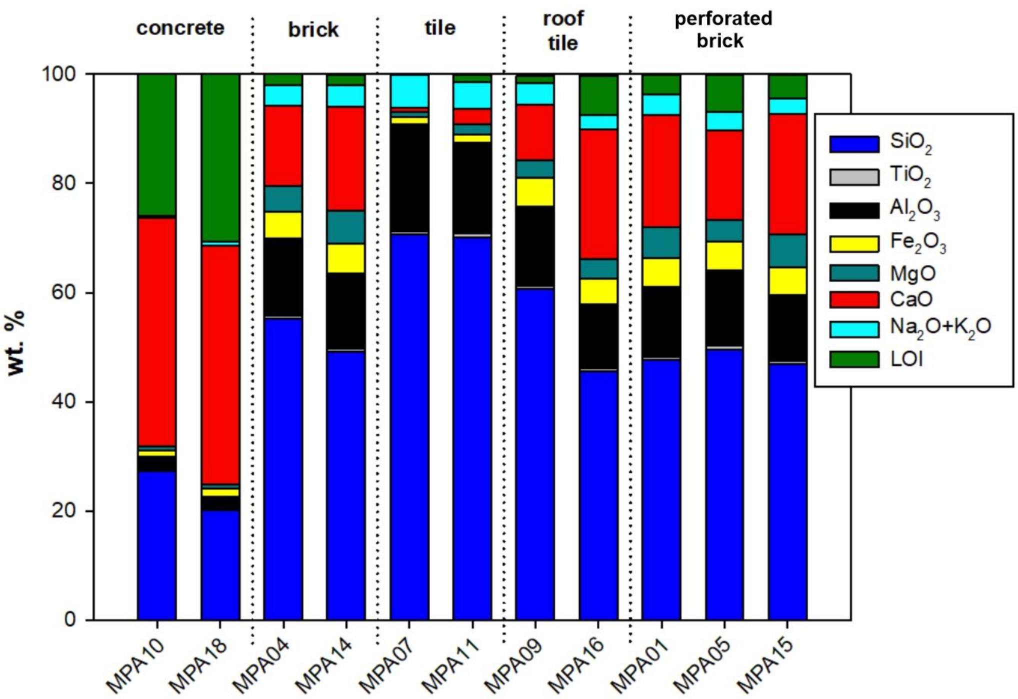

Fig. 3. Quantitative abundance of major oxides (wt.%) of the selected samples representative of distinct groups of CDW materials. Concrete are is in CaO and LOI (volatiles) and relatively poor in SiO_2, whereas bricks, tiles, roof tiles and perforated bricks are rich in SiO_2

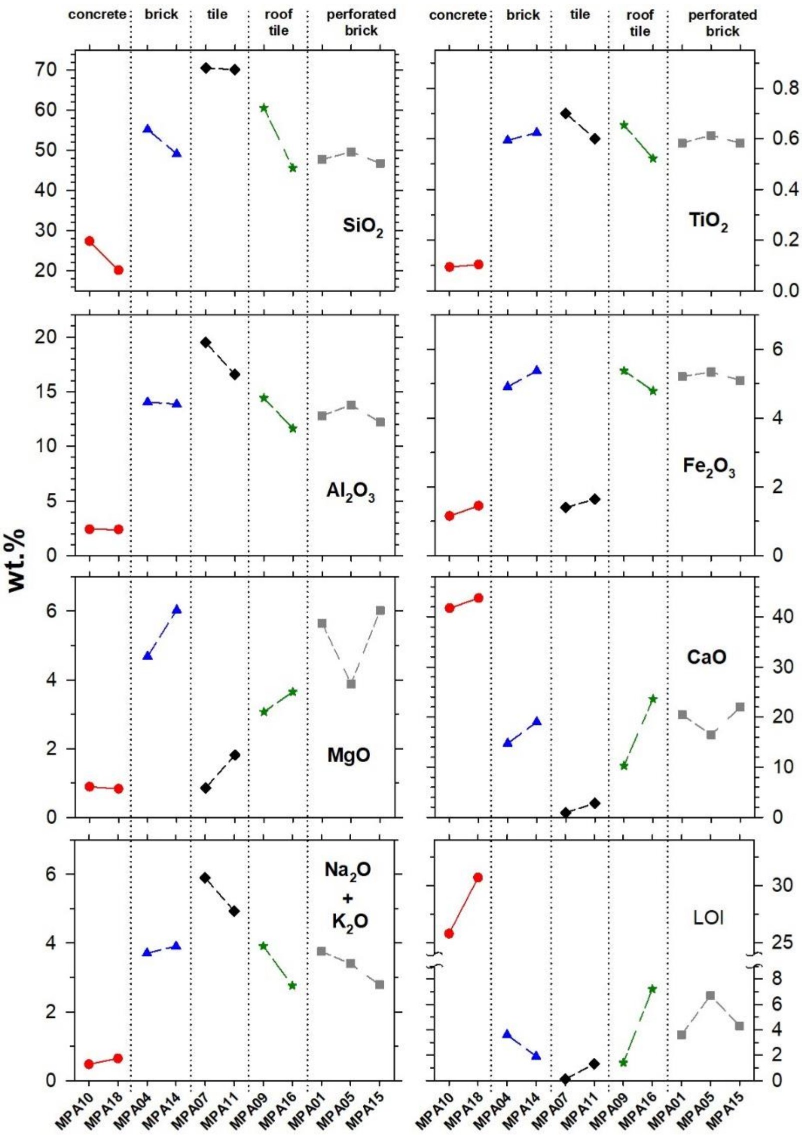

Fig. 4. Scatter plot of the results obtained from XRF analyses. Contents of major oxides among samples and groups. Some elements are plotted together as a function of their chemical characteristics.

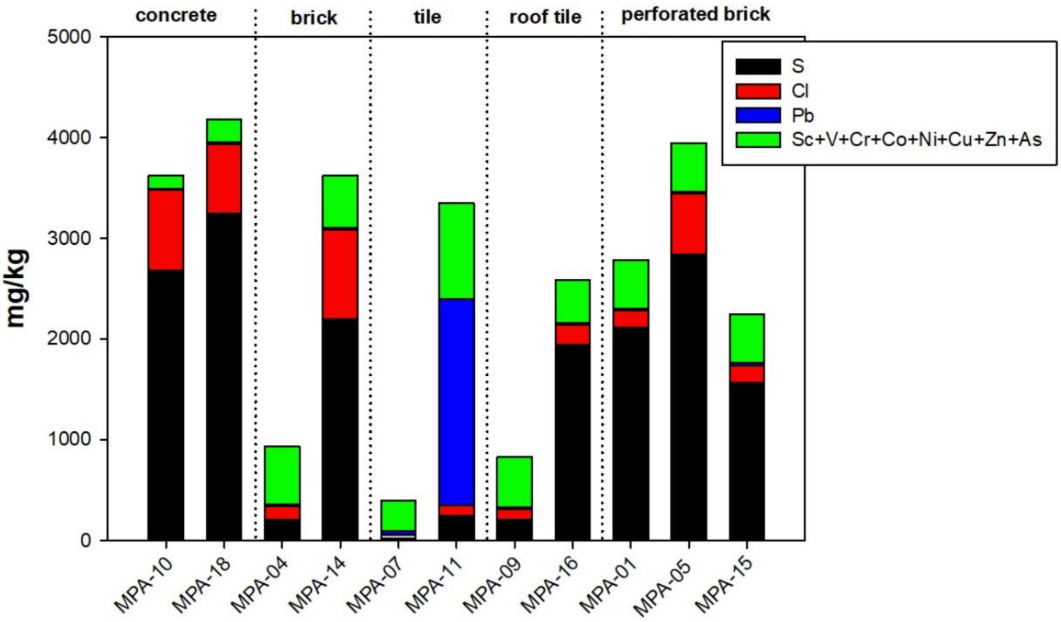

Fig. 5. Comparison of the abundance of minor and trace elements of samples and groups to highlight the most significant differences. Some minor and trace elements are plotted together as a function of their chemical characteristics.

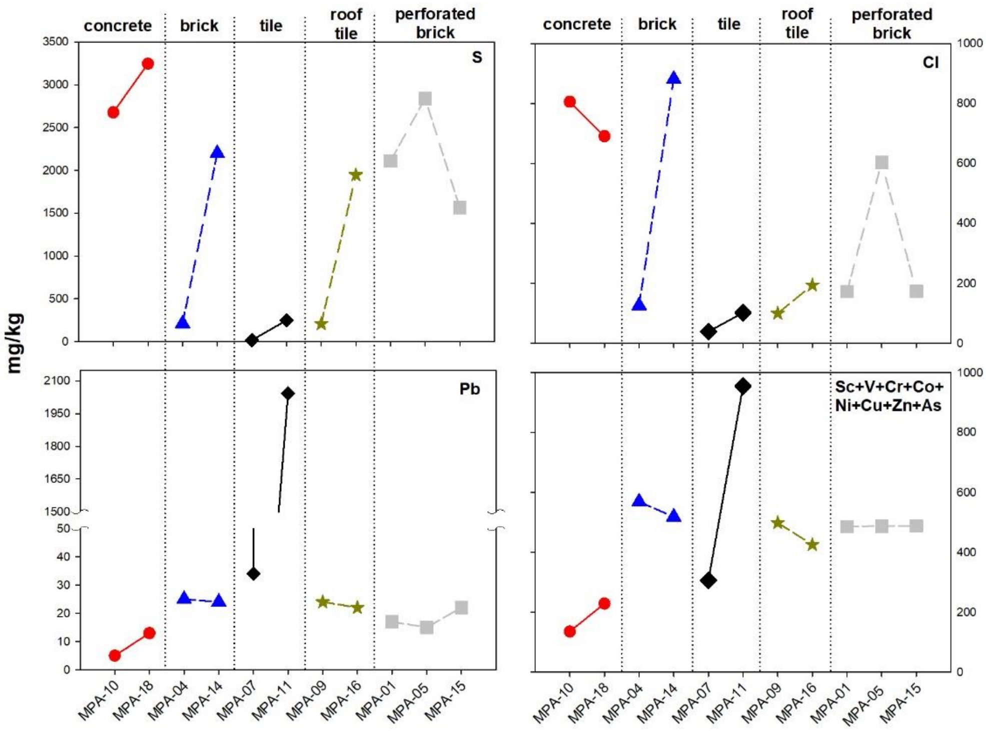

Fig. 6. Contents of minor and trace elements among samples and groups. Some elements are plotted together as a function of their chemical characteristics.

Overall, all the minor and trace element contents are lower than 1 wt.% (Fig. 5). The differences and similarities observed for major oxide bulk chemical compositions in and between CDW groups are not mirrored by the content of minor and trace elements (Tables S3 and S4 and Figs. 5, 6). For example, concrete shows a remarkable similarity with bricks and perforated bricks, especially for MPA-10, MPA-18, MPA-14 and MPA-05; the brick MPA-04 and the two perforated bricks MPA-01 and MPA-05 samples are very close in minor and trace element contents (Figs. 5, 6). By contrast, the two tiles MPA-07 and MPA-11 are similar to MPA-09 and to a lesser extent with the MPA-16 roof tiles (Figs. 5, 6).

The content of critical S and Cl are relatively high for both concrete samples (MPA-10 and MPA-18) and the brick MPA-14 and the perforated brick MPA-05 samples; the tiles and roof tiles are instead poor in S and Cl (Table S4 and Figs. 5, 6). Remarkably, the amount of Pb is extremely low for all samples except the MPA-11 tile that is exceptionally rich in Pb (Table S4 and Figs. 5, 6). Finally, the amount of Sc, V, Cr, Co, Ni, Cu, Zn and As metals is several hundreds of mg/kg; concrete contains the lowest contents (Table S4 and Figs. 5, 6).

Leachates. The possible release of dangerous chemical species by CDW is an important issue in terms of toxicological and environmental issues (Bianchini et al., 2020). The most significant and potentially harmful elements and their threshold values (according to the Italian norms) are reported in Table S5 as a function of the CDW groups; the most valuable metallic elements are also plotted in Fig. 7. The release of any element is invariably and by far lesser than 1 mg/l. According to the Italian legislation, only As and Cr in some samples are higher than the corresponding limits. In fact, both bricks, the MPA-07 tile and the MPA-15 perforated brick samples, have As contents higher than 0.01 mg/l; in parallel, the Cr content of the two concrete and the MPA-05 perforated bricks samples have significant higher amounts than the admissible 0.05 mg/l value (Table S5 and Fig. 7).

Discussion

The petrographic heterogeneity of CDW is the main limitation for their upcycling reuse. For instance, RAC (recycled aggregate concrete) prepared with masonry materials (MRA: masonry recycled aggregates) and/or the attached fraction of cement binders in RCA (recycled concrete aggregates) tend to have poorer performance than conventional concrete (e.g. de Brito et al., 2005; Evangelista et al., 2007; Gonçalves & de Brito, 2010; Agrela et al., 2011; Coelho & de Brito, 2013; Bravo et al., 2015; Bravo et al., 2020). In parallel, the quantification of the mesoscopic, physical and petrographic differences is critical for the possible elimination of a heterogeneous CDW, like that occurring under uncontrolled demolitions, illegal disposal and rubble from earthquakes (Martín-

Morales et al., 2011; Di Maria et al., 2013; Ulsen et al., 2013; Bonifazi et al., 2017a; Neto et al., 2017; Ambros et al., 2019).

The determination of the mesoscopic, physical, mineralogical and chemical attributes of single CDW samples from Abruzzo performed here unveils several aspects. The colour (appearance), texture, density, mineralogy and chemical composition show high to moderate similarities within each group (concrete, ornamental stone, brick, tile, roof tile and perforated bricks) (Figs. 2, 3, 4, S2). By contrast, the differences are clearer between different groups, especially between concrete and natural stone and the other four groups (Figs. 2, 3, 4, S2).

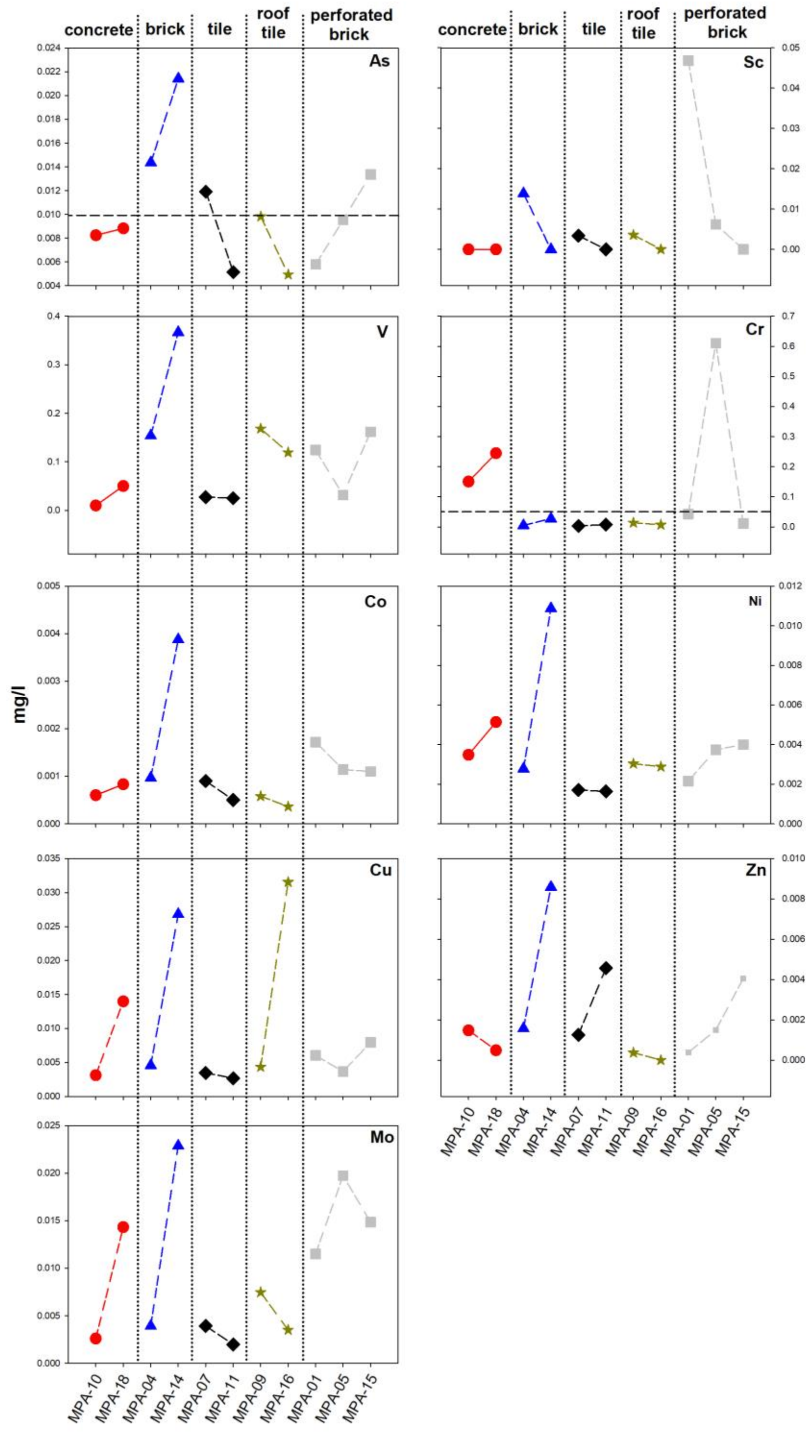

Fig. 7. Contents of As, Sc, V, Cr, Co, Ni, Cu, Zn and Mo in leachates. The black dotted line indicates the Italian Threshold Values of Heavy Metals (TVHM) (see Table S5)

Typical concrete, mortars and stone from Abruzzo are white to grey, whereas all the other masonry CDW are coloured, except the MPA-07 grey tile (Table S1 and Fig. S2). Similarly, concrete and stone have moderate to high density (2 to 2.7 g/cm^3), whereas the perforated bricks' density is always and markedly lower than 2 g/cm^3. The other groups are instead more scattered, with a tendency to be less than 2 g/cm^3 (Table S1); specifically, the MPA-04 (brick), MPA-17 (tile) and MPA-12 (roof tile) samples overlap the average density of concrete (2.2 ± 0.2 g/cm^3) (Table S1). All these mesoscopic features suggest that the separation of CDW from Abruzzo, as well as those from similar geographical and geological regions, can only be poorly enforced using processing based on density (e.g. Coelho & de Brito, 2013; Di Maria et al., 2013 and 2016; Ambros et al., 2017; Bonifazi et al., 2017a; Hu et al., 2019) but more efficiently with procedures based on colour (Gokyuu et al., 2011). Hence, an initial heterogeneous CDW from Abruzzo can be separated relatively well in two fractions using density and, especially, colour attributes: the first, enriched in concrete and stone, the second in masonry-rich CDW materials.

These mesoscopic (mainly colour) and physical differences between concrete and stone and masonry materials reflect petrographic attributes. The former are rich (> 50 wt.%) to exclusively (100 wt.%) made up of calcite and obviously present high values (> 50 wt.%) of CaO and LOI (volatile components), reflecting the high amount of CO_2 of the carbonate aggregates (Figs. 1, 2, 3). On the other hand, bricks, perforated bricks, tiles and roof tiles are calcite-poor or -free and rich in crystalline and non-crystalline silicate phases (Figs. 1, 2, 3). Thereby, the separation of concrete from masonry CDW materials in Abruzzo can be further enhanced by a separation based on chemical compositions (Serranti et al., 2015; Bonifazi et al., 2017b, 2018, 2019), since the former are CaO-rich and SiO_2-poor, while the latter show the inverse characteristics.

The amounts of the various crystalline phases in the CDW from Abruzzo are compared with those provided in four previous studies performed on CDW from the Veneto region in north-east of Italy (Panizza et al., 2018), central Spain (Frias et al., 2020), Portugal (Rodrigues et al., 2013) and southern part of Greece (Alexandridou et al., 2014). These investigations deal with either mixed CDW or selected groups like in here (Table S2). Overall, the typical crystalline phases solidified from the cement bindings fraction of concrete, i.e. ettringite, thaumasite, portlandite, etc., are undetected or detected with very low amounts (Table S2 and Fig. 2). The mineralogy of CDW concrete from Abruzzo is very similar to that analysed in southern Greece (Alexandridou et al., 2014) and relatively close to that coming from Veneto (Panizza et al., 2018). By contrast, the mixed CDW from Spain (Frias et al., 2020) and Portugal (Rodrigues et al., 2013) show a low to moderate amount of carbonates (calcite +

dolomite) (Table S2 and Fig. 2), probably reflecting the mixing of concrete with masonry materials, as well as different lithological features. Indeed, the Abruzzo, Veneto and southern Greece regions are extremely rich in carbonate rocks that were used to build most human structures.

Due to their crystalline and non-crystalline phases, concrete (and natural stone) and masonry CDW from Abruzzo are significantly different (Figs. 3, 4). Again, the former is enriched in CaO and LOI (CO_2) and poor in SiO_2, Al_2O_3 and alkalis (Table S3 and Fig. 4). A more robust reappraisal of the similarities and differences between CDW from different regions worldwide can be obtained through their chemical features. In Table S3, the most significant studies, for which quantitative chemical characterisation of CDW was provided, were reported. These data are compared in triangular diagrams in Fig. 8.

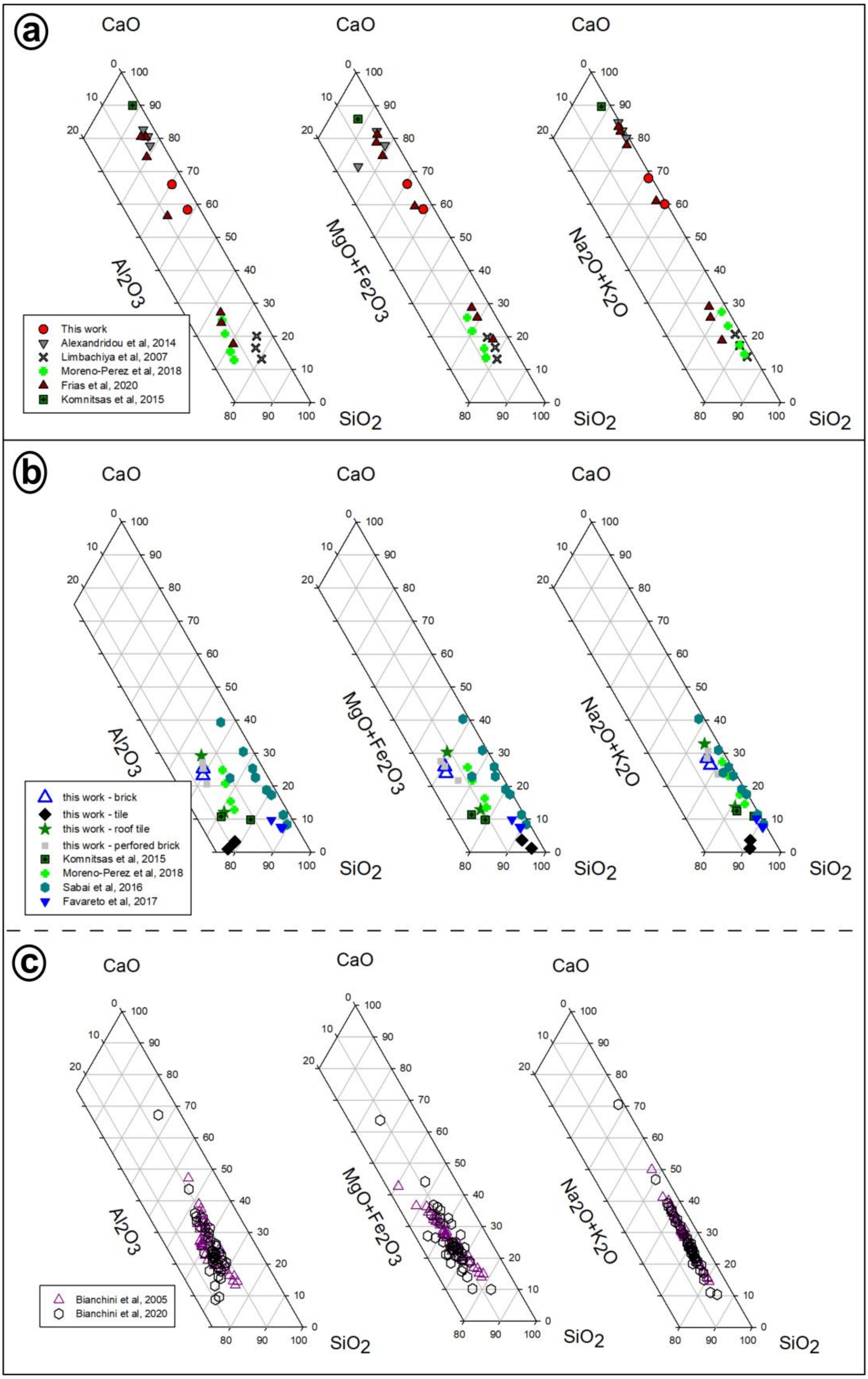

Fig. 8. Major chemical oxides of CDW from different provenance worldwide. a) CDW made of concrete; b-c) CDW made of masonry and ceramics. These data are reported in Table S3.

The concrete groups from Abruzzo and southern Greece (Alexandridou et al., 2014) are both very rich in CaO and poor in $SiO_2 + Al_2O_3$, in line with XRPD outcomes (Fig. 2); conversely, the three CDW concrete samples (RCA1, RCA2 and RCA3 in Table S3) from London (UK) (Limbachiya et al., 2007) are poor in CaO and rich in SiO_2. The former two groups again reflect the extremely high abundance of carbonate rocks in Central Italy and southern Greece, whereas those of Limbachiya et al. (2007) mirror the paucity of carbonate rocks around London. At the same time, all the CDW from other regions, made up of mixed CDW, have a content of CaO invariably lower than that of $SiO_2 + Al_2O_3$, $SiO_2 + MgO + Fe_2O_3$ and $SiO_2 + Na_2O + K_2O$ (Fig. 8). These features reflect both their mixed CDW signature and the scarcity of carbonate rocks from these areas. It is finally relevant to highlight that CDW from Abruzzo is strongly different from that sampled in Ferrara, Emilia-Romagna region. These two areas are located at a distance of only few hundreds of km, have been inhabited for thousands years and their architectural histories are close. Nevertheless, their construction materials are significantly different, due to the abundance of carbonates rocks in Abruzzo and their scarcity in the Po River plain settlements (Vola et al., 2011). Therefore, these outcomes strongly raise the necessity to characterise the petrography of CDW at a local level to identify their main chemical and mineralogical features, as well as to design sorting procedures based on their petrography.

Conclusion

As a general conclusion, areas rich in carbonate rocks, i.e. limestone, can be expected to share similar features of their CDW concrete such as: a relative high density, a whitish to pale grey colours, high amounts of calcite/dolomite crystalline phases, as well as being CaO- and CO_2-rich (Figs. 3, 8, S2). These aspects make CDW from Abruzzo and similar regions able to be sorted and separated in two main and relatively homogeneous concrete and masonry groups, *via* macroscopic colour investigation and whole chemical sorting procedures. Finally, the leaching test shows that some samples exceed the Italian Threshold Values of Heavy Metals (TVHM) limit (Italian Legislative Decree 152, 03/04/2006) for Cr and As (Table S5 and Fig. 7). These aspects are already reported for other CDW (Frias et al., 2002; Eštoková et al., 2012) and further highlight the necessity to characterise routinely the petrography and geochemistry, as well as the leachates, of CDW worldwide.

References

Agrela F., Sánchez de Juan M., Ayuso J., Geraldes V.L, Jiménez J.R., 2011. Limiting properties in the characterisation of mixed recycled aggregates for use in the manufacture of concrete. Construction and Building Materials, 25, 10, pp. 3950-3955.

Alexandridou C., Angelopoulos G. N., Coutelieris F. A., 2014. Physical, Chemical and mineralogical characterization of construction and demolition waste produced in Greece. International Scholarly and Scientific Research & Innovation, 8(9).

Ambros W.M., Sampaio C.H., Cazacliu B.G., Miltzarek G.L., Miranda L.R., 2017. Usage of air jigging for multi-component separation of construction and demolition waste. Waste Management, 60, pp. 75–83

Ambrós W.M., Sampaio C.H., Cazacliu B.G., Conceição P.N., dos Reis G.S., 2019. Some observations on the influence of particle size and size distribution on stratification in pneumatic jigs. Powder Technology, 342, pp. 594–606.

Blengini G. A., Garbarino E., 2010. Resources and waste management in Turin (Italy): the role of recycled aggregates in the sustainable supply mix. Journal of Cleaner Production, 18, pp. 1021–1030.

Bianchini G., Martucci A., Vaccaro C., 2002. Petro-archaeometric characterisation of "cotto ferrarese": bricks and terracotta elements from historic buildings of Ferrara. Per. Mineral., 71, special issue: Archaeometry and Cultural Heritage, 101-111.

Bianchini G., Marrocchino E., Tassinari R., Vaccaro C., 2005. Recycling of construction and demolition waste materials: a chemical–mineralogical appraisal. Waste Management, 25, pp. 149–159.

Bianchini G., Ristovski I., Milcov I., Zupac A., Natali C., Salani G. M., Marchina C., Brombin V., Ferraboschi A., 2020. Chemical Characterisation of Construction and Demolition Waste in Skopje City and Its Surroundings (Republic of Macedonia). Sustainability 12, 2055.

Boncio P., Amoroso S., Galadini F., Galderisi A., Iezzi G., Liberia F., 2020. Earthquake-induced liquefaction features in a late Quaternary fine-grained lacustrine succession (Fucino Lake, Italy): Implications for microzonation studies. Engineering Geology, 272, 105621.

Bonifazi G., Serranti S., Potenza F., Luciani V., Di Mario F., 2017a. Gravity packaging final waste recovery based on gravity separation and chemical imaging control. Waste Management, 60, pp. 50–55.

Bonifazi G., Palmieri R., Serranti S., 2017b. Concrete drill core characterization finalized to optimal dismantling and aggregates recovery. Waste Management, 60, pp 301–310.

Bonifazi G., Palmieri R., Serranti S., 2018. Evaluation of attached mortar on recycled concrete aggregates by hyperspectral imaging. Construction and Building Materials, 169, pp 835–842.

Bonifazi G., Capobianco G., Palmieri R., Serranti S., 2019. Hyperspectral imaging applied to the waste recycling sector. Spectroscopy Europe, 31, 2, pp 8-11.

Bravo M., de Brito J., Pontes J., Evangelista L., 2015. Mechanical performance of concrete made with aggregates from construction and demolition waste recycling plants. Journal of Cleaner Production, 99, pp. 59–74.

Bravo M., Duarte A. P. C., de Brito J., Evangelista L., Pedro D., 2020. On the development of a technical specification for the use of fine recycled aggregates from construction and demolition waste in concrete production. Materials, 13, 4228.

Cachim P.B., 2009. Mechanical properties of brick aggregate concrete. Construction and Building Materials, 23, pp. 1292–1297.

Chipera S.J. and Bish D.L., 2013. Fitting full X-Ray diffraction patterns for quantitative analysis: a method for readily quantifying crystalline and disordered phases. Advances in Materials Physics and Chemistry, 3, 47–53.

Chunshu, W., Mingcai, Y., Wenhua, Z., Qinghua, C., Tiexin, G., 1996. Chinese synthetic silicate and limestone certified reference materials for spectral analysis. Geostandard Newsletter. 20, 57–64.

Coelho A., de Brito J., 2013. Economic viability analysis of a construction and demolition waste recycling plant in Portugal e part I: location, materials, technology and economic analysis. Journal of Cleaner Production, 39, pp. 338-352.

Di Maria F., Micale C., Sordi A., Cirulli G., Marionni M., 2013. Urban mining: Quality and quantity of recyclable and recoverable material mechanically and physically extractable from residual waste. Waste Management, 33, pp. 2594–2599.

Di Maria F., Bianconi F., Micale C., Baglioni S., Marionni M., 2016. Quality assessment for recycling aggregates from construction and demolition waste: An image-based approach for particle size estimation. Waste Management, 48, pp. 344–352.

Ente Nazionale Italiano di Unificazione. UNI EN 12457—Part 2 (2004)—Characterisation of waste-leaching-compliance test for leaching of granular waste materials and sludges—Part 2: One stage batch test at a liquid to solid ratio of 10 l/kg for materials with particle size below 4 mm (without or with size reduction); Ente Nazionale Italiano di Unificazione: Milan, Italy, 2004.

Eštoková A., Palaščákováa L., Singovszkáb E., Holubb M., 2012. Analysis of the chromium concentrations in cement materials. Procedia Engineering, 42, pp. 123-130.

European Parliament. Directive 2008/98/CE of the European Parliament and of the Council of 19 November 2008 on Waste and Repealing Certain Directives. O. J. Eur. Union 2008, L312, 3–30. https://eur-lex.europa.eu/legal-content/EN/TXT/?uri=celex%3A32008L0098

Eurostat, 2017. Generation of Waste by Waste Category, Hazardousness and NACE Rev 2 Activity. https://appsso.eurostat.ec.europa.eu/nui/show.do?dataset=env_wasgen&lang=en

Evangelista L., de Brito J., 2007. Mechanical behaviour of concrete made with fine recycled concrete aggregates. Cement and Concrete Research, 29, 397–401.

Favaretto P., Hidalgo G.E.N., Sampaio C.H., de Almeida Silva R., Lermen R.T., 2017. Characterization and use of construction and demolition waste from south of brazil in the production of foamed concrete blocks. Applied Science, 7, 1090.

Frias M, Sánchez de Rojas MI, 2002. Total and soluble chromium, nickel and cobalt content in the main materials used in the manufacturing of Spain commercial cements. Cement and Concrete Composites, 32, pp. 435- 440.

Frias M., de la Villa R.V., Ramírez S.M., Carrasco L.F., Cociña E.V., Giménez R.G., 2020. Multi-technique characterization of a fine fraction of CDW and assessment of reactivity in a CDW/lime system. Minerals, 10, 590.

Gálvez-Martos J., Stylesb D., Schoenbergerd H., Zeschmar-Lahle B., 2018. Construction and demolition waste best management practice in Europe. Resources, Conservation & Recycling 136, 166–178.

Galli, P., Castenetto, S., Peronace, E., 2017. The macroseismic intensity distribution of the 30 October 2016 earthquake in Central Italy (Mw 6.6): Seismotectonic implications. Tectonics 36, 1–13.

Gazzulla Barreda, M.F., Rodrigo Edo, M., Orduña Cordero, M., Ventura Vaquer, M.J., 2016. Determination of minor and trace elements in geological materials used as raw ceramic materials. Boletín de la Sociedad Española de cerámica y vidrio 55, 185–196.

Giuliani L., Iezzi G., Vetere F.P., Behrens H., Mollo S., Cauti F., Ventura G., Scarlato P. (2020). Evolution of textures, crystal size distributions and growth rates of plagioclase, clinopyroxene, and spinel crystallized at variable cooling rates from a mid-ocean ridge basaltic melt. Earth Science Reviews, 204, 103165.

Gonçalves P., de Brito J., 2010. Recycled aggregate concrete (RAC) - Comparative analysis of existing specifications. Magazine of Concrete Research, 62(5), pp. 339–46.

Gokyuu, T., Nakamura, S., Ueno, T., Nakamura, M., Inoue, D., Yanagihara, Y., 2011. Sorting system for recycling of construction byproducts with Bayes' theorem-based robot vision. Journal of Robotics and Mechatronics, 23 (6), pp. 1066–1072.

Hu K., Chen Y., Naz F., Zeng C., Cao S., 2019. Separation studies of concrete and brick from construction and demolition waste. Waste Management, 85, pp. 396–404.

Hubbard C.R. and Snyder R.L., 1998. RIR - Measurement and use in quantitative XRD. Powder Diffraction, 3 (2), p. 74–77.

Komnitsas K., Zaharaki D., Vlachou A., Bartzas G., Galetakis M., 2015. Effect of synthesis parameters on the quality of construction and demolition wastes (CDW) geopolymers. Advanced Powder Technology, 26, pp. 368–376.

Johnson Q. and Zhou R.S., 2000. Checking and estimating RIR values. Advances in X-ray Analysis, 42, pp. 287–296.

Lachance G.R., Traill R.J., 1966. Practical solution to the matrix problem in X-ray analysis.

Canadian Journal of Spectroscopy, 11, pp. 43–48.

Merico A., Iezzi G., Pace B., Ferranti L., Cremona M., Scafa M., Cavallo A., Colella A., Nazzari m., Scarlato P. (2020). Grain size and grain size distribution of a lithified fault core in carbonates rocks using multi-scale image analysis: The example of the San Benedetto-Gioia dei Marsi fault (Central Italy). Journal of Structural Geology, 134, 104017.

Morales M., Zamorano M., Moyano, A.R., Espinosa I.V., 2011. Characterization of recycled aggregates construction and demolition waste for concrete production following the Spanish structural concrete code ehe-08. Construction and Building Materials, 25 (2), pp. 742–748.

Moreno-Pérez E., Hernández-Ávila J., Rangel-Martínez Y., Cerecedo-Sáenz E., Arenas-Flores A., Reyes-Valderrama M. I., Salinas-Rodríguez E., 2018. Chemical and mineralogical characterization of recycled aggregates from construction and demolition waste from Mexico City. Minerals, 8, 237.

Neto R.O., Gastineau P., Cazacliu B.G., Le Guen L., Paranhos R.S., Petter C.O., 2017. An economic analysis of the processing technologies in CDW recycling platforms. Waste Management, 60, pp. 277–289.

Panizza M., Natali M., Garbin E., Tamburini S., Secco M., 2018. Assessment of geopolymers with Construction and Demolition Waste (CDW) aggregates as a building material. Construction and Building Materials, 181, pp. 119–133.

Rodrigues F., Carvalho M. T., Evangelista L., de Brito J., 2013. Physical-chemical and mineralogical characterization of fine aggregates from construction and demolition waste recycling plants. Journal of Cleaner Production, 52, pp. 438-445.

Rukijkanpanich J., Thongchai N., 2019. Burned brick production from residues of quarrying process in Thailand. Journal of Building Engineering, 25, 100811.

Sabai S. M. M., Lichtenberg J. J., Egmond E. L., Florea M. V. M., Brouwers H.J.H., 2016. Construction and Demolition Waste Characteristics in Tanzania. Journal of the Open University of Tanzania, 23(1), pp 1-19.

Serranti S., Palmieri R., Bonifazi G., 2015. Hyperspectral imaging applied to demolition waste recycling: innovative approach for product quality control. Journal of Electronic Imaging, 24, 043003.

The Government of Italy. Legislative Decree 152/06 (2006) Norme in materia ambientale; Official Gazette n. 88; The Government of Italy: Rome, Italy, 2006. (In Italian)

Ulsen C., Kahn H., Hawlitschek G., Masini E. A., Angulo S. C., 2013. Separability studies of construction and demolition waste recycled sand. Waste Management, 33, pp. 656–662.

Vitale P., Arena N., Di Gregorio F., Arena U., 2017. Life cycle assessment of the end-of-life phase of a residential building. Waste Management, 60, pp. 311–321.

Vola G., Berrab M., Rondenab E. (2011). Petrographic quantitative analysis of ASR susceptible Italian aggregates for concrete. 13th Euroseminar on Microscopy Applied to Building Materials 14-18 June 2011, Ljubljana, Slovenia.

Walter J.M., Iezzi G., Albertini G., Gunter M.E., Piochi M., Ventura G., Jansen E., Fiori F. (2013). Enhanced crystal fabric analysis of a lava flow sample by neutron texture diffraction: a case study from the Castello d’Ischia dome. Geochemistry, Geophysics, Geosystems, 14(1), pp. 179-196.

Table S1. Mesoscopic and physical features of CDW samples from the Abruzzo region

groups	sample label	mescoscopic color bulk	mescoscopic color powder	texture	density (g/cm^3)
concrete	MPA-03	grey	white	porphyric	2.49
	MPA-10	grey	white	porphyric	2.03
	MPA-13	grey	havana	porphyric	2.24
	MPA-18	grey	havana	porphyric	2.02
natural stone	MPA-08	white	white	aphanitic	2.74
	MPA-19	grey	havana	porphyric	2.1
brick	MPA-02	havana	havana	porphyric	2.01
	MPA-04	havana	havana	porphyric	2.25
	MPA-14	havana	havana	aphanitic	1.7
tile	MPA-07	grey	grey	aphanitic	2.08
	MPA-11	havana	havana	aphanitic	1.83
	MPA-17	havana	havana	aphanitic	2.3
roof tile	MPA-09	fire-brick	red	aphanitic	2.09
	MPA-12	fire-brick	red	aphanitic	2.22
	MPA-16	ocher	havana	porphyric	1.71
perforated brick	MPA-01	havana	havana	aphanitic	1.82
	MPA-05	red	red	aphanitic	1.94
	MPA-15	ocher	havana	porphyric	1.73

Table S2. Crys							
study	geographical provenance	CDW type	sample labels	cc	do	other carbonates	qz
This study	Abruzzo, Central Italy	concrete	MPA-03	**88**	0	0	**12**
			MPA-10	**77**	0	0	**8**
			MPA-13	**68**	0	0	**27**
			MPA-18	**56**	0	0	**20**
		natural stone	MPA-08	**100**	0	0	0
			MPA-19	**100**	0	0	0
		brick	MPA-02	0	0	0	**47**
			MPA-04	0	0	0	**48**
			MPA-14	0	0	0	**20**
		tile	MPA-07	0	0	0	**70**
			MPA-11	0	0	0	**100**
			MPA-17	0	0	0	**71**
		roof tile	MPA-09	0	0	0	**47**
			MPA-12	**22**	0	0	**36**
			MPA-16	**37**	0	0	**42**
		perforated brick	MPA-01	0	0	0	**53**
			MPA-05	0	0	0	**75**
			MPA-15	0	0	0	**45**
xandridou et al, 20	Southern Greece	mixed CDW	G-N	**97**	0	0	0
			FG-N	**97**	0	0	0
			S-N	**96**	**3**	0	**1**
			Lab. RCA	**54**	**36**	0	**8**
			S(1) RCA 0/4	**75**	**5**	0	**7**
			S(1) RCA 4/31.5	**81**	**4**	0	**5**
Frias et al, 2020	Central Spain	mixed CDW	HsT	**24**	0	0	**48**
			HsC	**28**	0	0	**49**
			HsS	**16**	0	0	**58**
			HcG	**52**	0	0	**10**
			HcL	**40**	0	0	**14**
			HcV	**62**	0	0	**12**
odrigues et al, 201	Portugal	mixed CDW 0-4mm	TRI	**20**	0	0	**76**
			VAL	**5**	0	0	**52**
			AMB-M	**16**	0	0	**79**
			AMB-C	**18**	0	0	**71**
			ARV	**24**	0	0	**74**
			VIM-1	**21**	0	0	**66**
			VIM-2	**25**	0	0	**64**
			SRG-1	**12**	0	0	**75**
			SRG-2	**6**	0	0	**86**
			RTR	**6**	0	0	**69**
		mixed CDW	TRI	**37**	0	0	**55**

		63µm	VAL	**32**	0	0	**47**
			AMB-M	**42**	0	0	**51**
			AMB-C	**44**	0	0	**48**
			ARV	**38**	0	0	**57**
			VIM-1	**35**	0	0	**50**
			VIM-2	**48**	0	0	**44**
			SRG-1	**39**	0	0	**48**
			SRG-2	**24**	0	0	**69**
			RTR	**20**	0	0	**43**
Panizza et al, 2018	Veneto, northern Italy	concrete	<0.063	**29.4**	**28**	**1.5**	**9.6**
			0.063-0.0125	**27.4**	**29.1**	**1.5**	**12.6**
			0.125-0.25	**28.4**	**27.9**	**0.9**	**15.1**
			0.25-0.5	**28.9**	**22**	**1.2**	**18.7**
			0.5-1	**29.2**	**21.1**	**0.4**	**19.8**
			1-Feb	**28.4**	**27.4**	**0.5**	**18.8**
		brick	<0.063	**1**	**1.1**	0	**24.4**
			0.063-0.0125	**1.2**	**1.1**	0	**30**
			0.125-0.25	**1.8**	**2.1**	0	**29.9**
			0.25-0.5	**2.8**	**2.3**	0	**25.8**
			0.5-1	**2.5**	**2**	0	**24.9**
			1-Feb	**3.1**	**2.3**	0	**25.5**

Footnotes: cc: calcite, do: dolomite, other carbonates: carbonate crystalline phases different from c

talline phases and their semi-quantitative abundance (wt.%) in the CDW samples from the Abruzzo region and previous studies.

phase								
cri	pl	kf	cpx	il	bi	me	mu	kao
0	0	0	0	0	0	0	0	0
0	**15**	0	0	0	0	0	0	0
0	0	0	0	**5**	0	0	0	0
0	**19**	0	0	**5**	0	0	0	0
0	0	0	0	0	0	0	0	0
0	0	0	0	0	0	0	0	0
5	**28**	**8**	**9**	0	0	**3**	0	0
30	**4**	0	0	0	0	**3**	**15**	0
5	0	**15**	**44**	0	0	**7**	**9**	0
6	24	0	0	0	0	0	0	0
0	0	0	0	0	0	0	0	0
8	**11**	0	0	0	0	0	0	0
1	**22**	0	**28**	0	0	**2**	0	0
0	**11**	0	**7**	0	**4**	**20**	0	0
1	**5**	0	**8**	0	0	**7**	0	0
0	**11**	0	**12**	0	0	**24**	0	0
0	**7**	0	**14**	0	4	0	0	0
0	**14**	0	**26**	0	0	**15**	0	0
0	0	0	0	0	0	0	0	0
0	0	0	0	0	0	0	0	0
0	0	0	0	0	0	0	0	0
0	0	0	0	0	**1**	0	0	0
0	0	**3**	0	0	**4**	0	0	0
0	0	**3**	0	0	**3**	0	0	0
0	0	**8**	0	**4**	0	0	0	0
0	0	**6**	0	**6**	0	0	0	0
0	0	**10**	0	**4**	0	0	0	0
0	0	**11**	0	**10**	0	0	0	0
0	0	**13**	0	**12**	0	0	0	**10**
0	0	**10**	0	**7**	0	0	0	0
0	0	**2**	0	**1**	0	0	0	0
0	0	**35**	0	**8**	0	0	0	0
0	0	**4**	0	**1**	0	0	0	0
0	0	**10**	0	**1**	0	0	0	0
0	0	**2**	0	0	0	0	0	0
0	0	**13**	0	**1**	0	0	0	0
0	0	**10**	0	**1**	0	0	0	0
0	0	**11**	0	**1**	0	0	0	0
0	0	**7**	0	0	0	0	0	0
0	0	**20**	0	**6**	0	0	0	0
0	0	**7**	0	**1**	0	0	0	0

0	0	16	0	5	0	0	0	0
0	0	6	0	1	0	0	0	0
0	0	7	0	2	0	0	0	0
0	0	4	0	1	0	0	0	0
0	0	11	0	3	0	0	0	0
0	0	6	0	1	0	0	0	0
0	0	8	0	1	0	0	0	0
0	0	4	0	0	0	0	0	0
0	0	26	0	11	0	0	0	0
0	3	1.5	0	0	1.8	0	0	0
0	3.6	1.9	0	0	1.4	0	0	0
0	4	2.6	0	0	1.9	0	0	0
0	4.6	2.3	0	0	1.3	0	0	0
0	5.2	2.8	0	0	1.9	0	0	0
0	4.6	2.6	0	0	1.4	0	0	0
0	13.8	9.3	7.1	0	4.7	0	0	0
0	12.1	9.5	6.3	0	5.1	0	0	0
0	14.2	8.6	6.3	0	4.3	0	0	0
0	13.3	7.5	7.4	0	4.2	0	0	0
0	13.2	7.4	8.1	0	3.9	0	0	0
0	15.1	8.4	8.7	0	4.7	0	0	0

c and do, qz: quartz, cri: cristobalite, pl: plagioclase, kf: k-feldspar, cpx: clinopyroxene, il: illite, bi: biotit

gy	ettr	hema	port	thau	ncp
0	0	0	0	0	0
0	0	0	0	0	0
0	0	0	0	0	0
0	0	0	0	0	0
0	0	0	0	0	0
0	0	0	0	0	0
0	0	0	0	0	0
0	0	0	0	0	**0**
0	0	0	0	0	**0**
0	0	0	0	0	**0**
0	0	0	0	0	0
0	0	0	0	0	0
0	0	0	0	0	0
0	0	0	0	0	0
0	0	0	0	0	0
0	0	0	0	0	0
0	0	0	0	0	0
0	0	0	0	0	0
0	0	0	0	0	0
0	0	0	0	0	0
0	0	0	0	0	0
0	0	0	**1**	0	0
0	0	0	0	**6**	0
0	0	0	0	**4**	0
0	0	0	0	0	**16**
0	0	0	0	0	**11**
0	0	0	0	0	**12**
0	0	0	0	0	**17**
0	0	0	0	0	**11**
0	0	0	0	0	**9**
0	0	0	0	0	0
0	0	0	0	0	0
0	0	0	0	0	0
0	0	0	0	0	0
0	0	0	0	0	0
0	0	0	0	0	0
0	0	0	0	0	0
1	0	0	0	0	0
0	0	0	0	0	0
0	0	0	0	0	0
0	0	0	0	0	0

0	0	0	0	0	0
0	0	0	0	0	0
0	0	0	0	0	0
0	0	0	0	0	0
1	0	0	0	0	0
1	0	0	0	0	0
4	0	0	0	0	0
3	0	0	0	0	0
0	0	0	0	0	0
0.3	**0.9**	0	0	0	**34.8**
0.3	**1.1**	0	0	0	**21**
0.5	**1**	0	0	0	**17.7**
0.3	**1**	0	0	0	**19.7**
0.3	**0.5**	0	0	0	**18.8**
0.3	0	0	0	0	**16.3**
0.6	0	**3.3**	0	0	**34.6**
0.3	0	**2.9**	0	0	**31.5**
0.6	0	**2.8**	0	0	**29.5**
0.5	0	**3.1**	0	0	**33.1**
0.5	0	**3**	0	0	**34.6**
0.8	0	**2.6**	0	0	**29**

e, me: melilite, mu: mullite, kao: kaolinite, gy: gypsum, ettr: ettringite, hema: hematite, port: portlandite,

thau: thaumasite, ncp: non-crystalline phases(s).

Table S3. Major oxides (wt.%) abundances in sel					
study	geographical provenance	CDW type	Samples	SiO2	TiO2
This study	Abruzzo, Central Italy	concrete	MPA-10	**27.4**	0.1
			MPA-18	**20.1**	0.1
		brick	MPA-04	**47.7**	**0.6**
			MPA-14	**49.1**	**0.6**
		tile	MPA-07	**70.6**	**0.7**
			MPA-11	**70.1**	**0.6**
		roof tile	MPA-09	**60.6**	**0.7**
			MPA-16	**45.6**	**0.5**
		perforated brick	MPA-01	**47.7**	**0.6**
			MPA-05	**49.6**	**0.6**
			MPA-15	**46.8**	**0.6**
xandridou et al, 2	Southern Greece	concrete and natural stone	G-N	0.18	0.01
			FG-N	0.24	0.01
			S-N	0.46	0.01
			Lab. RCA	**8.55**	0.07
			S(1) RCA 0/4	**10.85**	0.11
			S(1) RCA 4/31.5	**8.33**	0.09
mbachiya et al, 20	London, United Kingdom	concrete and natural stone	PC	**20.6**	0.22
			Nat. sand	**97.03**	0.01
			RCA1	**65.37**	0.22
			RCA2	**68.43**	0.39
			RCA3	**63.61**	0.17
			Nat. Grav.	**88.54**	0.05
reno-Pérez et al, 2	Mexico city, Mexico	mixed CDW	Plant-Rec. Grav.	**49.41**	0.49
			Plant-Rec. Sand	**50.76**	**0.54**
			Lab. - Rec. Grav.	**55.75**	0.48
			Lab. - Rec. Sand	**56.98**	0.49
Sabai et al, 2016	Dar es Salaam, Tanzania	mixed CDW	DS	**71.8**	0.2
			DS2	**80.3**	0.35
			DS	**60.5**	0.26
			DM1	**43.12**	0.25
			DM	**58**	0.24
			DM	**64.5**	0.3
			CM	**54.5**	**0.62**
			CS	**70.6**	0.32
			100 CDW	**62.95**	0.32
			NCA	**14.1**	0.06
			NFA	**80**	0.35
Favareto et al, 201	Candiota, Brazil	mixed CDW	fine	**78.38**	0.24
			medium	**77.75**	0.23

				coarse	**73.05**	0.35
Frias et al, 2020	Central Spain	concrete		OPC	**14.22**	0.2
				HsT	**49.97**	0.28
				HsC	**49.22**	0.3
				HsS	**58**	0.3
				HcG	**9.34**	0.14
				HcL	**23.27**	0.39
				HcV	**12.1**	0.42
omnitsas et al, 201	Greece	concrete			**5.81**	0.03
		brick			**57.79**	**0.85**
		tile			**70.54**	**0.77**
ianchini et al, 200	Ferrara, Central Italy	mixed CDW	>4	TQ1 A	**38.57**	0.29
			4-Feb	TQ1 B	**34.01**	0.24
			2-0.6	TQ1 C	**47.32**	0.28
			0.6-0.125	TQ1 D	**60.2**	0.3
			0.125-0.075	TQ1 E	**39.96**	0.41
			<0.075	TQ1 F	**36.64**	0.42
		mixed CDW	>4	TQ2 A	**30.99**	0.16
			4-Feb	TQ2 B	**25.15**	0.17
			2-0.6	TQ2 C	**37.18**	0.24
			0.6-0.125	TQ2 D	**57.13**	0.3
			0.125-0.075	TQ2 E	**46.51**	**0.51**
			<0.075	TQ2 F	**40.34**	**0.5**
		mixed CDW	>4	TQ3 A	**34.12**	0.25
			4-Feb	TQ3 B	**47.43**	0.36
			2-0.6	TQ3 C	**47.68**	0.39
			0.6-0.125	TQ3 D	**58.87**	0.36
			0.125-0.075	TQ3 E	**43.03**	**0.53**
			<0.075	TQ3 F	**41.39**	**0.54**
		mixed CDW	>4	MD 2 A	**38.65**	0.29
			4-Feb	MD 2 B	**39.62**	0.32
			2-0.6	MD 2 C	**48.27**	0.36
			0.6-0.125	MD 2 D	**54.42**	0.38
			0.125-0.075	MD 2 E	**42.85**	**0.54**
			<0.075	MD 2 F	**42.1**	**0.53**
		mixed CDW	>4	MD 1 A	**42.95**	0.37
			4-Feb	MD 1 B	**45.71**	0.49
			2-0.6	MD 1 C	**49.15**	0.47
			0.6-0.125	MD 1 D	**53.6**	0.42
			0.125-0.075	MD 1 E	**45.66**	**0.52**
			<0.075	MD 1 F	**42.41**	**0.54**
		mixed CDW	>4	MD 3 A	**39.24**	0.38
			4-Feb	MD 3 B	**43.16**	0.38
			2-0.6	MD 3 C	**43.16**	0.38
			0.6-0.125	MD 3 D	**53.3**	0.36
			0.125-0.075	MD 3 E	**42.1**	**0.5**

				<0.075	MD 3 F	**41.54**	**0.54**
			mixed CDW	>4	FN1 A	**37.45**	0.32
				4-Feb	FN1 B	**41.25**	0.35
				2-0.6	FN1 C	**49.84**	0.42
				0.6-0.125	FN1 D	**59.56**	0.38
				0.125-0.075	FN1 E	**50.41**	**0.55**
				<0.075	FN1 F	**48.46**	**0.57**
			mixed CDW	>4	FN2 A	**35.44**	0.28
				4-Feb	FN2 B	**39.7**	0.35
				2-0.6	FN2 C	**47.34**	0.39
				0.6-0.125	FN2 D	**55.62**	0.38
				0.125-0.075	FN2 E	**45.05**	**0.57**
				<0.075	FN2 F	**44.51**	**0.57**
Bianchini et al, 202	Skopje, Republic of Macedonia	mixed CDW			AF01	**37.06**	0.45
					AF02	**43.88**	0.41
					AF03	**54.1**	**0.58**
					AF04	**59.83**	**0.91**
					AF05	**43.26**	0.36
					AF06	**38.53**	0.49
					AF07	**58.3**	**0.76**
					AF08	**53.89**	**0.71**
					AF09	**14.55**	**0.55**
					AF10	**48.02**	**0.67**
					AF11	**47.87**	0.35
					AF12	**48.47**	**0.5**
					AF13	**43.26**	0.39
					AF14	**40.38**	**0.52**
					AF15	**49.32**	**0.5**
					AF16	**36.43**	0.45
					AF17	**47.02**	**0.53**
					AF18	**45.47**	**0.58**
					AF19	**48.94**	**0.59**
					AF20	**49.55**	**0.59**
					AF21	**51.31**	**0.56**
					AF22	**49.07**	**0.57**
					AF23	**32.2**	0.37
					AF24	**38.94**	0.48
					AF25	**52.16**	**0.67**
					AF26	**42.85**	**0.54**
					AF27	**40.29**	0.42
					AF28	**45.57**	**0.54**
					AF29	**49.34**	**0.64**
					AF30	**52.11**	**0.58**
					AF31	**52.42**	**0.62**
					AF32	**50.31**	**0.55**
					AF33	**51.12**	**0.62**

			AF34	**41.73**	0.49
			AF35	**49.24**	**0.53**
			AF36	**40.45**	**0.5**
			AF37	**45.92**	**0.57**
			AF38	**47.36**	**0.6**
			AF39	**45.93**	**0.61**

lected CDW samplesof CDW samples from the Abruzzo region and previous studies.

oxides (wt.%)								
Al2O3	Fe2O3	MnO	MgO	CaO	Na2O	K2O	P2O5	L.O.I.
2.4	**1.2**	0.1	**0.9**	**41.7**	0.2	0.2	0	**25.8**
2.4	**1.4**	0	**0.8**	**43.7**	0.2	0.4	0	**30.7**
12.8	**5.2**	0.1	**5.6**	**20.5**	**1.3**	**2.5**	0.1	**3.6**
13.9	**5.4**	0.1	**6**	**19**	**1.1**	**2.8**	0.1	**1.9**
19.5	**1.4**	0	**0.9**	**0.9**	**4.6**	**1.3**	0.1	0.1
16.6	**1.6**	0	**1.8**	**2.8**	**1.4**	**3.5**	0.1	**1.3**
14.4	**5.4**	0.1	**3.1**	**10.3**	**1.6**	**2.3**	0.1	**1.4**
11.6	**4.8**	0.1	**3.6**	**23.6**	**1.1**	**1.6**	0.1	**7.2**
12.8	**5.2**	0.1	**5.6**	**20.5**	**1.3**	**2.5**	0.1	**3.6**
13.8	**5.3**	0.1	**3.9**	**16.4**	**1**	**2.4**	0.1	**6.7**
12.2	**5.1**	0.1	**6**	**22**	**1.1**	**1.7**	0.1	**4.3**
0.05	0.04	0.01	0.34	**55.09**	0	0.02	0.03	**43.72**
0.08	0.06	0.01	0.37	**54.93**	0	0.02	0.04	**43.89**
0.13	0.08	0.01	0.38	**54.59**	0	0.02	0.05	**43.85**
1.34	**0.72**	0.04	**7.13**	**41.13**	0.12	0.19	0.03	**40.08**
2.03	**1.13**	0.02	**0.83**	**45.17**	0.13	0.24	0.02	**38.76**
1.65	**0.98**	0.02	**0.73**	**47.61**	0.08	0.17	0.02	**39.66**
5.47	**3.31**	0.06	**2.26**	**62.5**	**0.65**	**1.71**	0.21	**1.64**
0.34	0.1	0	**0.65**	0.26	0.16	0.01	0.02	**1.41**
5.33	**2.16**	0.05	**1.91**	**13.93**	**1.19**	**0.61**	0.11	**9.12**
5.49	**2.4**	0.05	**2.84**	**11.19**	**0.94**	**0.62**	0.1	**7.56**
3.57	**2.03**	0.06	**2.62**	**16.86**	**0.87**	**0.51**	0.49	**9.19**
1.21	**0.76**	0.02	0.42	**5.33**	0.33	0.31	0.08	**2.95**
8.44	**3.99**	0	**1.78**	**19.11**	0	**1.3**	0	0
9.25	**4.4**	0	**1.78**	**15.76**	0	**1.56**	0	0
10.52	**4.59**	0	**1.76**	**9.78**	0	**1.53**	0	0
10.84	**4.21**	0	**1.77**	**12.33**	0	**1.51**	0	0
1.6	0.4	0	0.2	**15.4**	0.1	0.2	0	**10.1**
1.57	0.48	0.02	0.15	**10.4**	0.15	0.27	0.02	**6.29**
2.32	0.26	0.03	0.28	**21.3**	0.31	0.45	0.04	**14.25**
3.16	**0.81**	0.04	0.43	**30**	0.48	0.65	0	**21.06**
2.35	**0.64**	0.02	0.43	**26.4**	0.19	0.71	0.06	**10.96**
1.92	**0.58**	0.03	0.28	**15.4**	0.31	0.37	0.03	**16.28**
8.21	**4.07**	0.1	**2.25**	**18.1**	**1.63**	**0.82**	0.12	**9.58**
1.72	**0.51**	0.02	0.18	**6.6**	0.1	0.17	0.01	**19.77**
2.86	**0.98**	0.04	**0.53**	**19.23**	0.42	0.45	0.04	**12.18**
0.94	0.35	0.02	**0.68**	**46.6**	0.09	0.11	0.08	**36.97**
1.93	**0.57**	0.02	0.21	**18**	0.12	0.19	0.02	0
3.39	**1.3**	0.06	**1.23**	**6.53**	0	**0.84**	0.06	**6.96**
3.74	**1.39**	0.05	**1.23**	**6.72**	0	**0.93**	0.04	**7.13**

4.83	**1.96**	0.06	**1.38**	**8.43**	0	**1.15**	0.06	**7.71**
2.89	**3.7**	0.1	**0.93**	**69.81**	0.33	**0.76**	0.14	**3.22**
8.98	**2.3**	0.4	**1.37**	**18.65**	**0.8**	**3.35**	0.11	**11.5**
8.01	**2.19**	0.03	**1.58**	**21.38**	**0.63**	**2.61**	0.12	**12.9**
9.56	**2.12**	0.03	**1.11**	**14.48**	**0.9**	**3.83**	0.1	**8.69**
2.88	**1.2**	0.09	**1.12**	**50.32**	0.18	0.47	0.03	**33.2**
6.58	**2.3**	0.05	**0.78**	**38.66**	0.41	**1.07**	0.08	**25.7**
3.78	**2.49**	0.06	**0.92**	**45.93**	0.25	**0.72**	0.09	**32.4**
1.49	**0.75**	0.01	**4.21**	**65.42**	**0.57**	**1.26**	**0.73**	**21.59**
14.95	**6**	0.05	**4.75**	**8.79**	**1.03**	**2.8**	0.23	**1.89**
9.8	**5.39**	0.06	**4.46**	**8.78**	0	**1.37**	0	0.23
7.26	**2.87**	0.11	**5.27**	**21.74**	**0.86**	**1.43**	0.15	**21.44**
6.04	**2.94**	0.14	**5.09**	**23.96**	**0.71**	**1.1**	0.21	**25.55**
7.64	**2.95**	0.12	**3.75**	**17.64**	**1.08**	**1.57**	0.21	**17.45**
8.75	**2.82**	0.1	**2.78**	**11.6**	**1.53**	**1.84**	0.17	**9.92**
8.39	**3.72**	0.14	**2.91**	**20.76**	**0.92**	**1.58**	0.35	**20.85**
8.6	**3.86**	0.14	**3.14**	**22.04**	**0.82**	**1.6**	0.42	**22.31**
5.55	**1.82**	0.07	**7.71**	**23.32**	**0.96**	**1.35**	**0.72**	**27.35**
4.5	**1.43**	0.06	**8.97**	**26.52**	**0.55**	**0.9**	0.29	**31.44**
6.51	**2.09**	0.08	**6.12**	**21.57**	**0.93**	**1.48**	**0.67**	**23.13**
8.55	**2.66**	0.09	**3.37**	**12.61**	**1.48**	**1.87**	**0.6**	**11.33**
9.07	**3.68**	0.12	**3.81**	**16.67**	**1.23**	**1.77**	**1.17**	**15.45**
8.93	**3.68**	0.12	**4.21**	**19.15**	**1.09**	**0.72**	**1.41**	**18.84**
6.4	**2.65**	0.11	**4.77**	**22.78**	**0.8**	**1.05**	0.31	**26.77**
8.07	**3.6**	0.12	**3.68**	**18.03**	**0.87**	**1.5**	**0.66**	**15.69**
9.31	**3.67**	0.11	**3.63**	**17.49**	**0.99**	**1.79**	**0.76**	**14.18**
9.62	**3.16**	0.1	**3.16**	**11.71**	**1.53**	**1.89**	**0.5**	**9.1**
10.88	**4.52**	0.14	**3.48**	**18.34**	**0.86**	**1.8**	**0.95**	**15.47**
10.4	**4.35**	0.14	**3.48**	**18.73**	**0.88**	**1.7**	**0.76**	**17.63**
7.26	**3.09**	0.12	**4.67**	**22.8**	**0.94**	**1.31**	0.21	**20.66**
7.92	**3.44**	0.12	**4.32**	**21.53**	**0.87**	**1.48**	0.26	**20.13**
9.15	**3.14**	0.11	**3.63**	**16.95**	**1.09**	**1.8**	0.31	**14.92**
9.59	**3.31**	0.1	**3.28**	**14.1**	**1.38**	**1.92**	0.27	**11.24**
10.85	**4.36**	0.13	**3.49**	**18.68**	**0.87**	**1.86**	0.49	**15.89**
10.55	**4.24**	0.13	**3.48**	**18.66**	**0.9**	**1.77**	0.49	**17.16**
8.77	**3.58**	0.12	**4.63**	**19.24**	**1.06**	**1.6**	0.23	**17.45**
11.27	**4.32**	0.12	**4.22**	**15.39**	**0.91**	**2.04**	**0.5**	**15.03**
10.96	**4.25**	0.12	**3.95**	**14.6**	**1.03**	**2.04**	**0.5**	**12.93**
10.11	**3.63**	0.11	**3.31**	**13.97**	**1.27**	**2**	0.43	**11.16**
10.12	**4.22**	0.12	**3.45**	**16.87**	**1.03**	**1.84**	**0.54**	**15.63**
10.31	**4.48**	0.13	**3.6**	**18.01**	**0.9**	**1.88**	**0.61**	**17.13**
9	**3.62**	0.14	**4.51**	**21.83**	**0.9**	**1.66**	0.2	**18.51**
9.25	**3.59**	0.12	**3.91**	**19.94**	**1.02**	**1.82**	0.21	**16.61**
9.25	**3.59**	0.12	**3.91**	**19.94**	**1.02**	**1.82**	0.21	**16.61**
9.04	**3.17**	0.1	**3.23**	**15.32**	**1.3**	**1.82**	0.21	**12.09**
10.58	**4.29**	0.13	**3.46**	**20.01**	**0.9**	**1.8**	0.37	**15.87**

10.72	**4.46**	0.13	**3.52**	**19.42**	**0.91**	**1.8**	0.37	**16.59**
7.35	**3.09**	0.11	**4.99**	**22.47**	**0.85**	**1.24**	0.21	**21.92**
8.42	**3.41**	0.11	**4.84**	**18.89**	**0.92**	**1.49**	0.22	**20.1**
9.86	**3.88**	0.11	**3.59**	**14.44**	**1.11**	**1.83**	0.29	**14.63**
9.59	**3.3**	0.1	**3**	**10.65**	**1.5**	**1.89**	0.29	**9.8**
10.32	**4.24**	0.12	**3.52**	**13.95**	**1.23**	**1.81**	0.34	**13.5**
10.56	**4.28**	0.12	**3.73**	**14.47**	**1.17**	**1.8**	0.37	**14.48**
6.89	**2.91**	0.11	**5.49**	**23.14**	**0.82**	**1.24**	0.25	**23.45**
8.01	**3.16**	0.11	**4.56**	**20.74**	**0.94**	**1.5**	0.39	**20.55**
9.09	**3.57**	0.11	**3.89**	**16.45**	**1.14**	**1.79**	0.43	**15.82**
9.49	**3.27**	0.1	**3.35**	**12.74**	**1.43**	**1.92**	0.33	**11.36**
11.46	**4.48**	0.13	**3.72**	**16.65**	**0.96**	**1.97**	**0.56**	**14.45**
11.07	**4.28**	0.12	**3.77**	**16.71**	**1**	**1.82**	**0.57**	**15.57**
8.36	**3.56**	0.09	**3.4**	**25.6**	**0.98**	**1.45**	0.12	**18.93**
8.24	**2.41**	0.07	**3.4**	**22.04**	**1.48**	**1.12**	0.11	**16.85**
10.88	**3.77**	0.08	**2.99**	**14.02**	**1.05**	**1.92**	0.11	**10.5**
16.53	**3.96**	0.05	**1.51**	**7.3**	**1**	**2.13**	0.09	**6.7**
8.57	**2.41**	0.06	**3.4**	**23.71**	**0.99**	**1.46**	0.09	**15.67**
8.64	**3.77**	0.09	**2.73**	**25.41**	**1.13**	**1.53**	0.17	**17.5**
14.83	**5.15**	0.14	**4.31**	**7.76**	**1.51**	**2.68**	0.15	**4.41**
13.86	**5.07**	0.15	**3.76**	**10.21**	**1.39**	**2.52**	0.12	**8.3**
3.46	**2.07**	0.03	**4.49**	**36.93**	0.46	0.38	0.07	**37.02**
12.41	**4.84**	0.12	**5.46**	**13.13**	**1.72**	**2.39**	0.18	**11.07**
8.26	**2.09**	0.05	**3.22**	**20.01**	**1.51**	**1.17**	0.15	**15.33**
10.55	**3.8**	0.08	**3.77**	**16.31**	**1.19**	**1.8**	0.1	**13.42**
10.94	**3.62**	0.06	**4.28**	**16.7**	**1.28**	**1.59**	0.2	**17.66**
9.07	**3.93**	0.1	**3.29**	**23.16**	**1.12**	**1.53**	0.17	**16.72**
10.16	**3.51**	0.07	**2.39**	**16.79**	**1.14**	**1.76**	0.1	**14.26**
8.47	**3.76**	0.1	**4.4**	**22.68**	**0.98**	**1.43**	0.11	**21.19**
10.16	**3.84**	0.07	**4.76**	**16.37**	**1.29**	**1.72**	0.14	**14.08**
9.46	**3.9**	0.16	**3.52**	**17.34**	**0.98**	**1.37**	0.14	**17.08**
10.25	**3.13**	0.07	**4.18**	**16.83**	**1.21**	**1.64**	0.09	**13.07**
9.58	**4.59**	0.16	**3.31**	**17.86**	**1.05**	**1.78**	0.09	**11.43**
8.16	**4.08**	0.1	**4.41**	**15.31**	**1.53**	**1.79**	0.25	**12.48**
8.32	**4.06**	0.1	**4.6**	**16.79**	**1.29**	**1.72**	0.28	**13.2**
6.64	**3.14**	0.07	**2.75**	**30.16**	**0.96**	**1.1**	0.17	**22.46**
7.77	**3.43**	0.08	**7.94**	**18.61**	**1.09**	**1.39**	0.25	**20.02**
11.65	**5.04**	0.13	**3.65**	**12.25**	**1.5**	**2.11**	0.18	**10.66**
9.63	**3.98**	0.09	**4.95**	**13.88**	**1.02**	**1.49**	0.25	**21.32**
7.55	**3.35**	0.09	**3.06**	**25.25**	**1.06**	**1.35**	0.13	**17.46**
8	**4.17**	0.1	**5.57**	**18.54**	**1.16**	**1.55**	0.21	**14.59**
10.3	**4.67**	0.11	**4.05**	**15.04**	**1.28**	**1.97**	0.22	**12.38**
9	**3.84**	0.09	**3.86**	**14.72**	**1.62**	**1.63**	0.18	**12.37**
11.24	**4.57**	0.1	**4.78**	**11.62**	**1.28**	**1.96**	0.14	**11.27**
8.8	**3.62**	0.09	**3.57**	**15.83**	**1.56**	**1.83**	0.25	**13.6**
10.51	**4.32**	0.11	**3.66**	**14.2**	**1.56**	**2.02**	0.22	**11.67**

7.15	**3.6**	0.09	**4.28**	**22.38**	**1.43**	**1.57**	0.25	**17.02**
8.59	**3.95**	0.1	**4.18**	**17.77**	**1.66**	**1.74**	0.17	**12.07**
7.93	**3.83**	0.09	**6.24**	**18.12**	**1.17**	**1.31**	0.23	**20.13**
9.46	**3.81**	0.08	**3.97**	**17.77**	**1.26**	**1.7**	0.19	**15.28**
9.55	**4.33**	0.1	**3.85**	**17.31**	**1.39**	**1.72**	0.19	**13.59**
9.41	**4.36**	0.1	**5.85**	**15.03**	**1.44**	**1.81**	0.33	**15.13**

tot
100
100
100
100
100
100
100
100
100
100
100
100
100
100
100
100
100
100
100
100
100
100
100
100
100
100
100
100
100
100
100
100
100
100
100
100
100
100

100
100
100
100
100
100
100
100
100
100
100
100
100
100
100
100
100
100
100
100
100
100
100
100
100
100
100
100
100
100
100
100
100
100
100
100
100
100
100
100
100
100
100
100
100
100

100
100
100
100
100
100
100
100
100
100
100
100
100
100
100
100
100
100
100
100
100
100
100
100
100
100
100
100
100
100
100
100
100
100
100
100
100
100
100
100
100
100
100
100
100
100

100
100
100
100
100
100

Table S4. Minor and trace elements (mg/kg) in the CDW samples from the Abru							
elements	concrete		brick		tile		roof
	MPA-10	MPA-18	MPA-04	MPA-14	MPA-07	MPA-11	MPA-09
S	2677	3246	210	2200	17	248	208
Cl	806	691	126	882	39	102	100
Sc	3	2	12	12	9	7	11
Cr	25	42	119	117	62	99	127
Ni	18	26	80	68	16	26	77
Co	5	3	18	10	14	10	19
As	7	udl	12	10	9	udl	8
Zn	28	47	175	133	115	720	106
Cu	31	70	40	49	10	19	42
V	19	39	113	120	71	74	109
Pb	5	13	25	24	34	2043	24

zzo region.

tile	perforated brick		
MPA-16	MPA-01	MPA-05	MPA-15
1946	2108	2841	1564
194	173	604	174
14	12	12	12
89	109	110	100
52	57	60	66
18	16	17	16
11	23	13	16
94	104	86	139
60	42	45	47
88	124	145	91
22	17	15	22

Table S5. Content of elements in leachates in the CDW samples from tl							
mg/l	TVHM	concretes		bricks		tiles	
	(IT)	MPA-10	MPA-18	MPA-04	MPA-14	MPA-07	MPA-11
As	0.01	0.008	0.009	**0.014**	**0.021**	**0.012**	0.005
Sc	-	n.d.	n.d.	0.014	n.d.	0.003	n.d.
V	-	0.01	0.05	0.154	0.367	0.027	0.025
Cr	0.05	**0.151**	**0.245**	0.005	0.027	0.003	0.008
Co	0.05	0.001	0.001	0.001	0.004	0.001	0.001
Ni	0.02	0.003	0.005	0.003	0.011	0.002	0.002
Cu	1	0.003	0.014	0.005	0.027	0.003	0.003
Zn	3	0.001	0	0.002	0.009	0.001	0.005
Mo	-	0.003	0.014	0.004	0.023	0.004	0.002

Footnotes. n.d.: not determined.

he Abruzzo region.				
roof tiles		perforated bricks		
MPA-09	MPA-16	MPA-01	MPA-05	MPA-15
0.01	0.005	0.006	**0.01**	**0.013**
0.004	n.d.	0.047	0.006	n.d.
0.168	0.119	0.124	0.032	0.162
0.014	0.007	0.043	**0.611**	0.011
0.001	0	0.002	0.001	0.001
0.003	0.003	0.002	0.004	0.004
0.004	0.032	0.006	0.004	0.008
0	n.d.	0	0.001	0.004
0.007	0.004	0.012	0.02	0.015

Supplementary figures

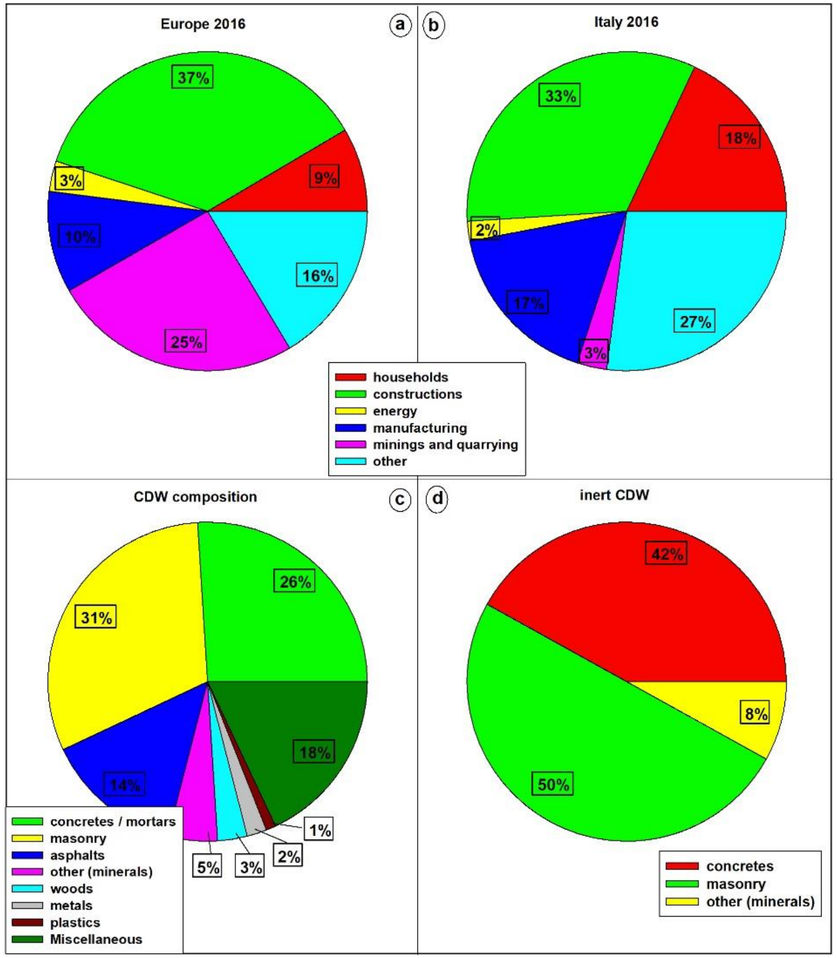

Fig. S1. Shows the amount (wt. %) of wastes in Europe and Italy (a and b) as a function of activity (http://ec.europa.eu/eurostat/statistics-explained/index.php/Waste_statistics); types of material in a general CDW (c) and types of material in the ceramic-like and inert CDW fraction (d) in the EU (or similarly in Italy). “Masonry” includes bricks and perforated bricks, “other mineral” refers to tiles, roof tiles and stone, while “miscellaneous” considers textiles, RAEE, glass, dredging materials and others.

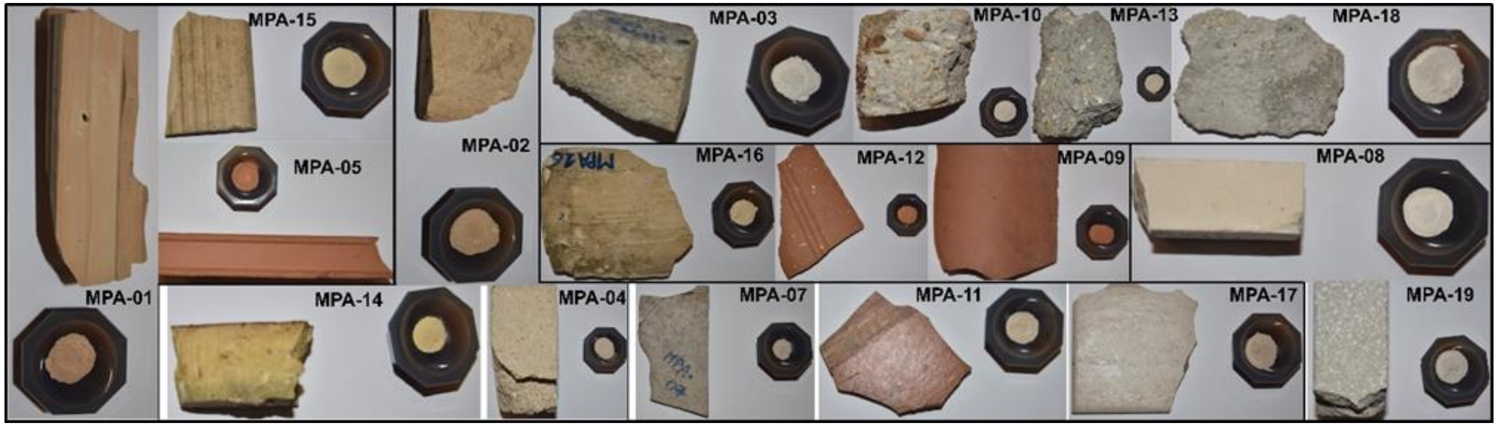

Fig. S2. Mesoscopic (bulk and as-received) samples of CDW collected in the Abruzzo region (Central Italy), and resulting powder samples

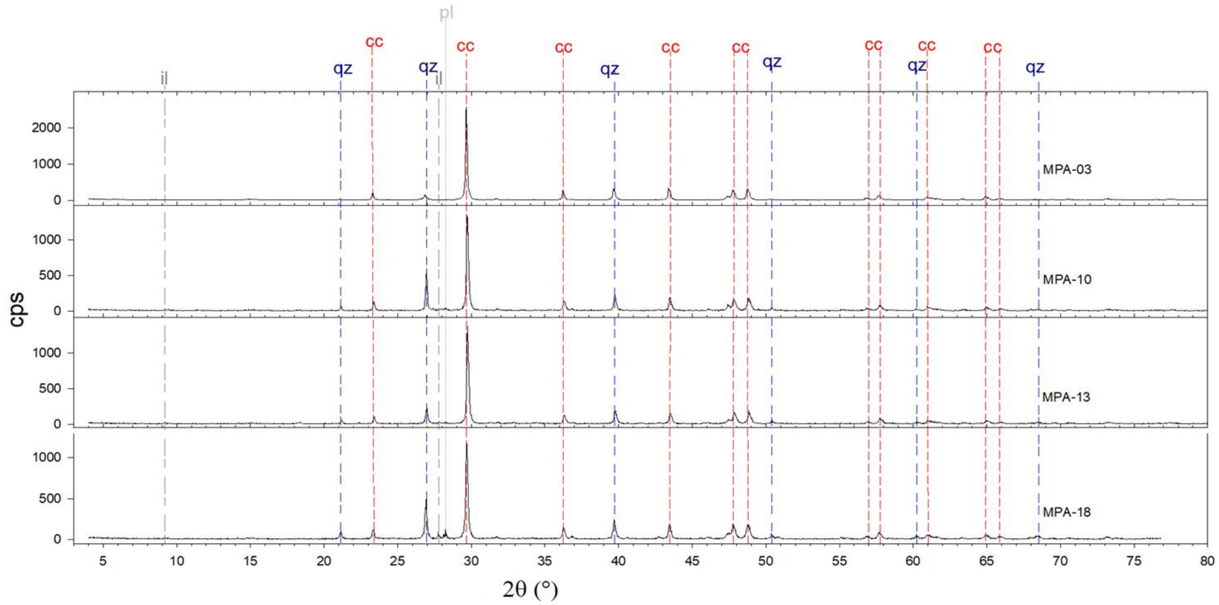

Fig. S3a. Stacked XRPD patterns of concrete (Table 1S); the vertical lines correspond to Bragg reflections of crystalline standards of the ICSD database; cps indicates count per second; calcite (cc), quartz (qz), illite (il), plagioclase (pl).

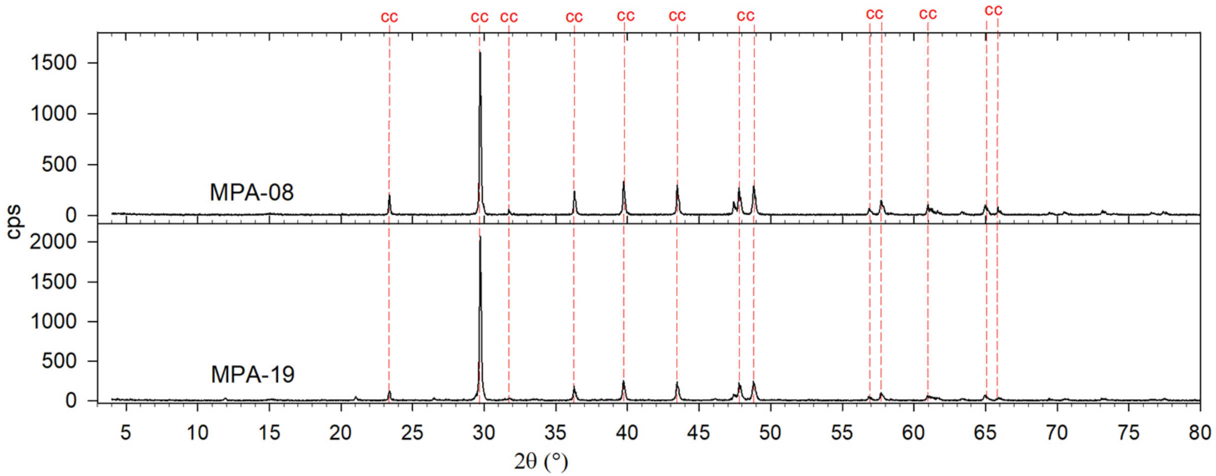

Fig. S3b. Stacked XRPD patterns of natural stone (Table 1S); the vertical lines correspond to Bragg reflections of crystalline standards of the ICSD database; cps indicates count per second; calcite (cc).

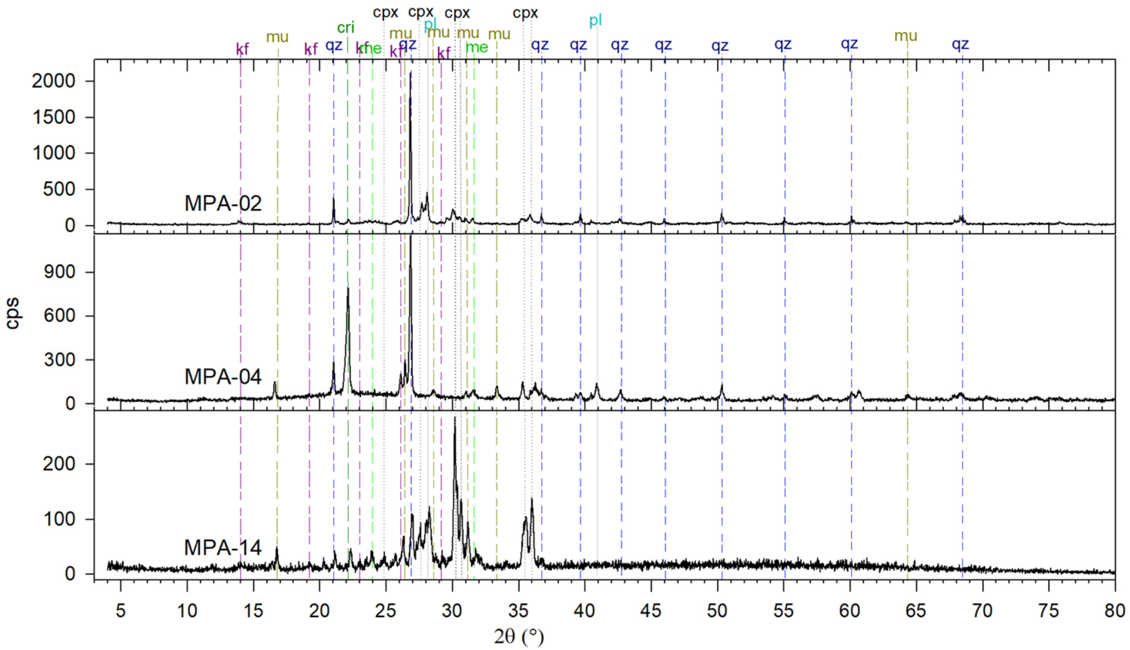

Fig. S3c. Stacked XRPD patterns of bricks (Table 1S); the vertical lines correspond to Bragg reflections of crystalline standards of the ICSD database; cps indicates count per second; calcite (cc), quartz (qz), plagioclase (pl), cristobalite (cri), k-feldspar (kf), clinopyroxene (cpx), mullite (mu), melilite (me).

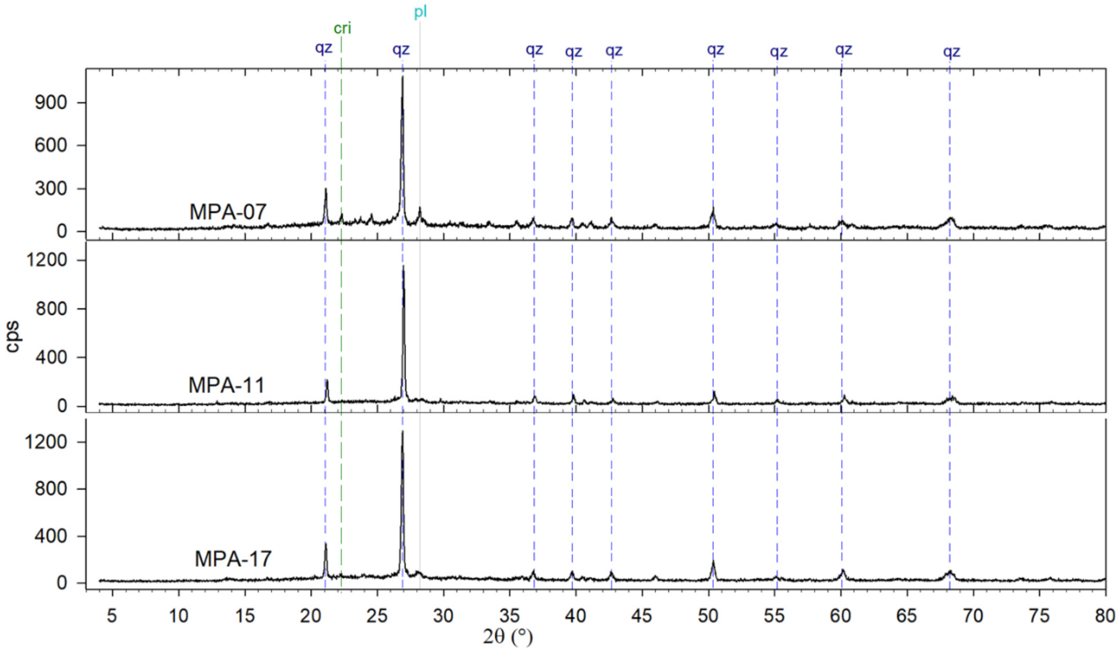

Fig. S3d. Stacked XRPD patterns of tiles (Table 1S); the vertical lines correspond to Bragg reflections of crystalline standards of the ICSD database; cps indicates count per second; quartz (qz), plagioclase (pl), cristobalite (cri).

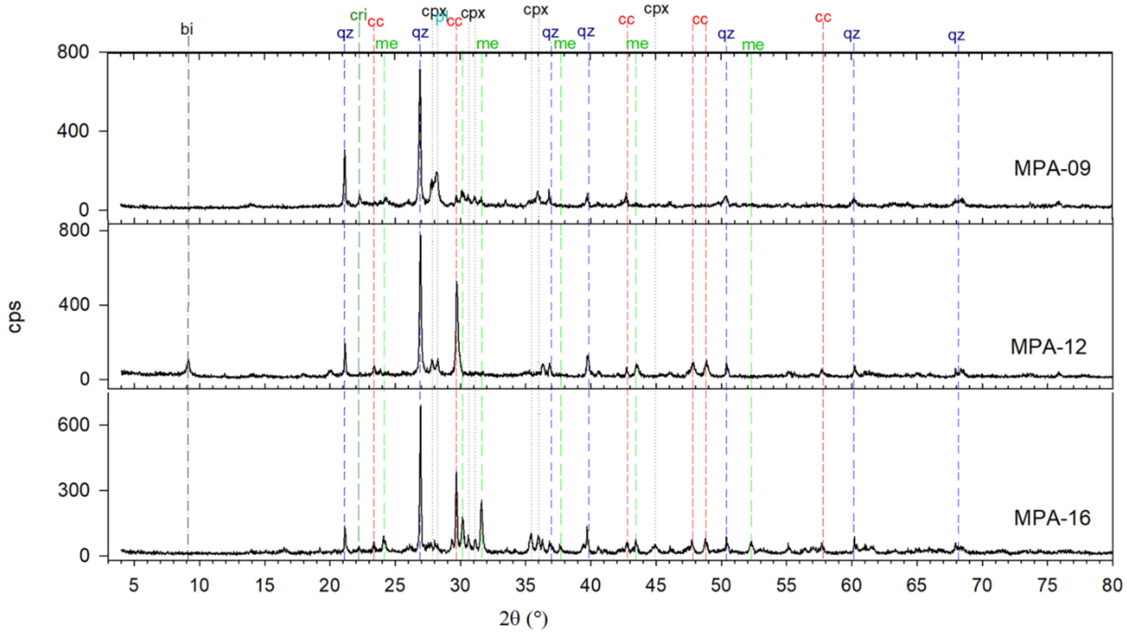

Fig. S3e. Stacked XRPD patterns of roof tiles (Table 1S); the vertical lines correspond to Bragg reflections of crystalline standards of the ICSD database; cps indicates count per second; calcite (cc), quartz (qz), plagioclase (pl), cristobalite (cri), clinopyroxene (cpx), melilite (me), biotite (bi).

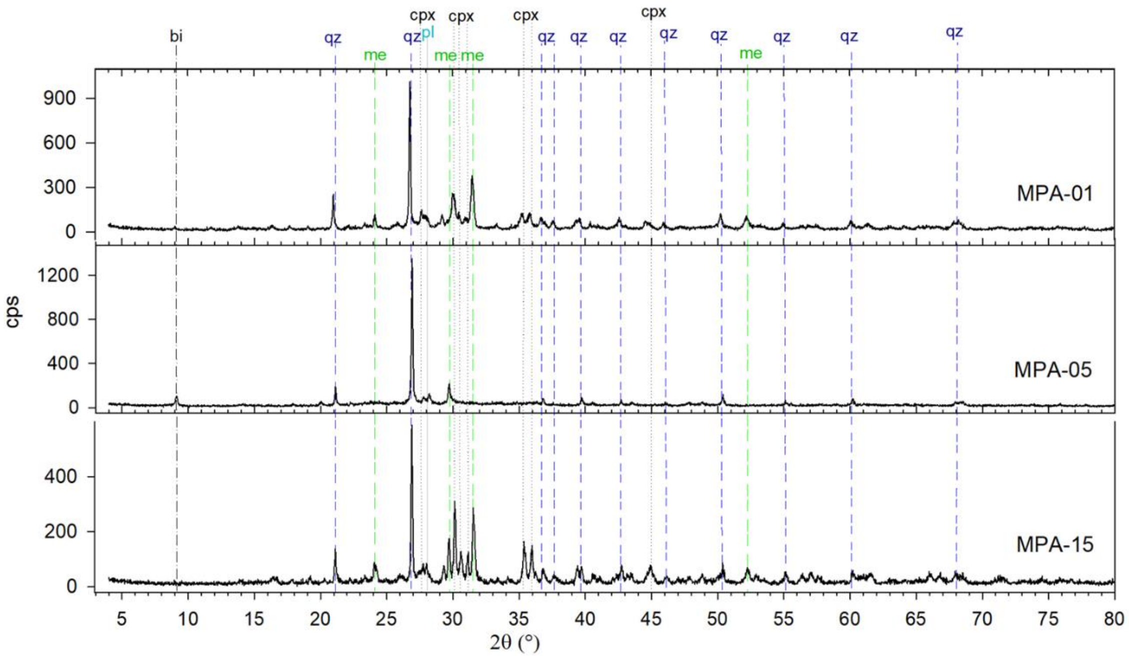

Fig. S3f. Stacked XRPD patterns of performed bricks (Table 1S); the vertical lines correspond to Bragg reflections of crystalline standards of the ICSD database; cps indicates count per second; calcite (cc), quartz (qz), plagioclase (pl), clinopyroxene (cpx), melilite (me), biotite (bi).

Declaration of competing interest

The authors have no financial and personal relationships with other people or organizations regarding the treatment of these issues and data.